

Synthesis and Design of Graphene- Based Nanostructure as an Electromagnetic Wave Absorbing Material

Submitted to the Graduate School of Natural and Applied Sciences
in partial fulfillment of the requirements for the degree of

Master of Science

in Materials Science and Engineering

by

Gülperi Feyza YAVUZ

ORCID 0000-0001-9493-627X

July, 2023

This is to certify that we have read the thesis **Synthesis and Design of Graphene-Based Nanostructure as an Electromagnetic Wave Absorbing Material** submitted by **Gülperi Feyza YAVUZ**, and it has been judged to be successful, in scope and in quality, at the defense exam and accepted by our jury as a MASTER'S THESIS.

APPROVED BY:

Advisor: **Assoc. Prof. Dr. Fethullah GÜNEŞ**
İzmir Kâtip Çelebi University

Committee Members:

Assoc. Prof. Dr. Levent AYDIN
İzmir Kâtip Çelebi University

Assist. Prof. Dr. Mustafa EROL
Dokuz Eylül University

Date of Defense: July 5, 2023

Declaration of Authorship

I, **Gülperi Feyza YAVUZ**, declare that this thesis titled **Synthesis and Design of Graphene-Based Nanostructure as an Electromagnetic Wave Absorbing Material** and the work presented in it are my own. I confirm that:

- This work was done wholly or mainly while in candidature for the Master's degree at this university.
- Where any part of this thesis has previously been submitted for a degree or any other qualification at this university or any other institution, this has been clearly stated.
- Where I have consulted the published work of others, this is always clearly attributed.
- Where I have quoted from the work of others, the source is always given. This thesis is entirely my own work, with the exception of such quotations.
- I have acknowledged all major sources of assistance.
- Where the thesis is based on work done by myself jointly with others, I have made clear exactly what was done by others and what I have contributed myself.

Date: 30.05.2023

Synthesis and Design of Graphene-Based Nanostructure as an Electromagnetic Wave Absorbing Material

Abstract

The progress of electronic information technology brings along some problems caused by electromagnetic (EM) waves. For this reason, electromagnetic absorber materials have drawn attention recently for application areas such as electronic, defense stealth technology, and satellite communication systems. These materials provide magnetic and dielectric properties which induce interaction with incident electromagnetic radiation. These materials provide magnetic and dielectric loss properties which induce interaction with incident electromagnetic radiation. Therefore, EM wave absorber materials should have characteristics of thin-film thickness, lightweight, broad bandwidth, and strong absorptivity for high efficiency. Since the traditional EM wave absorber materials are not to be able to meet the demand, carbon-based nanostructures, such as graphene derivatives and carbon nanotubes (CNT), have become strong alternative materials. Graphene derivatives can provide the required properties for EM wave absorption because of their superior properties, such as high thermal conductivity, tensile strength, flexibility, low thermal expansion coefficient, and lightweight. However, at that point, graphene may not be enough for the efficient microwave absorption feature alone. Thus, graphene and derivatives are mainly used with some supportive nanostructures such as ZnO, MnO₂, and NiO. In addition, hybrid nanomaterials enhance microwave absorption properties by increasing the impedance matching of the structure. Especially high surface/volume ratio and interconnected 3D

network structure of graphene-based foams provide a wide working area with adaptable properties such as broadband absorption and strong desorption. The graphene foam will be synthesized in this thesis to examine the EM wave absorption property. Additionally, graphene foam will be combined with the most suitable nanostructure to be synthesized via the hydrothermal method. It is estimated that the combination process will be increased the impedance matching of the structure. Thus, in microwave frequency technology, unlike traditional materials which are widely studied, the use of graphene is aimed to increase the electromagnetic wave absorption capacity. Furthermore, in this study, the design of the experiment, providing statistical time and cost-saving for determining optimum conditions with the less experimental process, will be carried out.

Keywords: graphene, nanocomposite, electromagnetic wave absorption, hydrothermal method

Elekromanyetik Dalga Soğurucu bir Malzeme Olarak Grafen Tabanlı Nanoyapı Sentezi ve Tasarımı

ÖZ

Elektronik bilgi teknolojisinin gelişmesi, elektromanyetik (EM) dalgaların neden olduğu bazı sorunları da beraberinde getirmektedir. Bu nedenle elektromanyetik soğurucu malzemeler son zamanlarda elektronik, savunma gizli teknoloji, uydu haberleşme sistemleri gibi uygulama alanlarında dikkat çekmektedir. Bu malzemeler, gelen elektromanyetik radyasyonla etkileşime neden olan manyetik ve dielektrik kayıp mekanizmaları sağlar. Bu nedenle, EM dalga soğurucu malzemeler, yüksek verimlilik için ince film kalınlığı, hafiflik, geniş bant genişliği ve güçlü soğurma özelliklerine sahip olmalıdır. Geleneksel EM dalga soğurucu malzemeler talebi karşılayamadığı için grafen türevleri ve karbon nanotüpler (CNT) gibi karbon bazlı nanoyapılar güçlü alternatif malzemeler haline gelmiştir. Grafen türevleri, yüksek termal iletkenliğe sahip, yüksek mukavemet, esneklik ve hafiflik gibi üstün özelliklerinden dolayı EM dalga absorpsiyonu için gerekli özellikleri sağlayabilir. Ancak bu noktada grafen, etkili mikrodalga absorpsiyon özelliği için tek başına yeterli olmayabilir. Bu nedenle, grafen ve türevleri temel olarak ZnO, MnO₂ ve NiO gibi bazı destekleyici nanoyapılarla birlikte kullanılır. Ek olarak, hibrit nanomalzemeler, yapının empedans eşleşmesini artırarak mikrodalga absorpsiyon özelliklerini geliştirir. Özellikle grafen bazlı köpüklerin yüksek yüzey/hacim oranı ve birbirine bağlı üç boyutlu ağ yapısı, geniş bant absorpsiyonu ve güçlü desorpsiyon gibi uyarlanabilir özellikleri ile geniş bir çalışma alanı sağlar. Bu tezde EM dalga soğurma özelliğini incelemek için grafen

köpük/MnO₂ nanotel hibrit yapısı sentezlenecektir. Hibrit yapının, empedans uyumunu artıracığı öngörülmüştür. Böylece mikrodalga frekans teknolojisinde, üzerinde çokça çalışılan geleneksel malzemelerden farklı olarak grafen kullanımı ile elektromanyetik dalga soğurma kapasitesinin arttırılması amaçlanmaktadır. Ayrıca bu çalışmada daha az deneysel işlemle optimum koşulların belirlenmesi için istatistiksel zaman ve maliyet tasarrufu sağlayan deney tasarımı gerçekleştirilmiştir.

Anahtar Kelimeler: grafen, nanokompozit, elektromanyetik dalga soğurma, hidrotermal yöntem

To my loving family...

Acknowledgment

First of all, I would like to thank my esteemed advisor, Assoc. Prof. Dr. Fethullah Güneş for his guidance and support during my graduate studies.

I would like to thank Assoc. Prof. Dr. Mustafa Erol, Prof. Dr. Merih Palandöken, and Assist. Prof. Dr. Ahmet Aykaç for their support and helps. I also express my gratitude to Evren Egesoy and Dr. Seher Küçük due to their support and friendship. Moreover, I am thankful to Dr. Koray Kara and Dr. Hakan Bilgili for the project collaboration.

I would like to express my deepest appreciation to Assoc. Prof. Dr. Levent Aydın for his guidance and encouragement all the time in any situation.

Additionally, I would like to recognize The Scientific and Technological Research Council of Turkey (TÜBİTAK) – Science Fellowships and Grand Programmes Department (BİDEB) because I was funded within the scope of the ‘2210/C National MSc/MA Scholarship Program in the Priority Fields in Science and Technology’ during the term 2021/1.

Moreover, I would like to thank İzmir Kâtip Çelebi University-Scientific Research Projects Unit for their financial support to this thesis study through projects with numbers 2021-GAP-MÜMF-0042 / 2022-TYL-FEBE-0019 and Dokuz Eylül University Center for Fabrication and Applications of Electronic Materials (EMUM).

Besides, I would like to express my most profound appreciation to Dr. Hazal Gergeroğlu, Dr. Melih Savran, Gülsüm Ersü, İpek Yoldaş, and Hande Parlak for their invaluable support and friendship during my MSc studies.

Additionally, I want to express my gratitude to Kemal Bartu Aydın '*forty ways from Sunday*' for all the support he has given me and valuable suggestions in my journey.

Finally, I sincerely thank Semiha Yavuz, Mehmet Yavuz, and Būşra Yavuz for their patience, support, and prayers during this time. I am particularly grateful for their encouragement on whatever I decided to go for.

Gūlperi Feyza YAVUZ

Table of Contents

Declaration of Authorship.....	ii
Abstract	iii
Öz.....	v
Acknowledgment	viii
Table of Contents	x
List of Figures	xii
List of Tables.....	xiii
List of Abbreviations.....	xiv
1. Introduction.....	1
2. Electromagnetic Wave Absorption – Materials Interactions.....	3
2.1 Electromagnetic Wave Absorption	3
2.2 Graphene-Based Electromagnetic Wave Absorbing Materials.....	6
2.2.1 Graphene-Based Magnetic Metal Nanocomposites.....	7
2.2.2 Graphene-Based Ferrite Nanocomposites.....	7
2.2.3 Graphene-Based Polymer Nanocomposites.....	8
2.2.4 Graphene-Based Ceramic Nanocomposites.....	8
2.2.5 Graphene-Based Multicomponent Nanocomposites	9
2.2.6 Graphene-Based Carbon Material Nanocomposites.....	10
2.3 CVD-Based Graphene Foam and Electromagnetic Wave Absorption	11
2.4 Electromagnetic Wave Absorption of Manganese Oxide.....	13
2.5 Motivation.....	14
3. Materials and Method	16

3.1	Graphene Foam Synthesis via Chemical Vapor Deposition Method.....	16
3.2	Seeding Layer Application of Graphene Foam.....	16
3.3	Experimental Design.....	17
3.4	Graphene Foam/ α -MnO ₂ NWs Synthesis via Hydrothermal Method	18
3.5	Characterization	19
4.	Result and Discussion	21
4.1	Scanning Electron Microscopy (SEM)	21
4.2	X-Ray Diffraction Analysis (XRD)	26
4.3	Raman Spectroscopy	28
4.4	Vector Network Analysis (VNA).....	30
5.	Conclusion.....	34
	References	38
	Appendices	47
	Appendix A	48
	Publications from the Thesis	48
	Curriculum Vitae	49

List of Figures

Figure 2.1	The Electromagnetic Spectrum.....	4
Figure 2.2	GF/ α -MnO ₂ hybrid structures experimental steps.....	15
Figure 3.1	Graphical abstract of the MnO ₂ NW growth via hydrothermal method.	19
Figure 4.1	x100 SEM images, GF, F-1, F-2, F-3, F-4, F-5, F-6, F-7, F-8.....	23
Figure 4.2	x1.00k SEM images, GF, F-1, F-2, F-3, F-4, F-5, F-6, F-7, F-8.....	24
Figure 4.3	x10.00k SEM images F-1, F-2, F-3, F-4, F-5, F-6, F-7, F-8.....	25
Figure 4.4	x500 SEM images of F-5 and F-7 respectively.....	26
Figure 4.5	x20.00k SEM images of F-5 and F-7 respectively.....	26
Figure 4.4	XRD graph of the GF and GF/ α -MnO ₂	27
Figure 4.5	XRD graph of the all GF/ α -MnO ₂ samples.....	28
Figure 4.6	Raman spectrum of the GF/ α -MnO ₂ samples.....	29
Figure 4.7	SE Total of all GF/MnO ₂ samples.....	31
Figure 4.8	SE Absorption of all GF/MnO ₂ samples.....	32
Figure 4.9	SE Reflection of all GF/MnO ₂ samples.....	32

List of Tables

Table 3.1	Variables utilized in full factorial design with their levels	18
Table 3.2	Experimental design results	18
Table 4.1	Raman spectrum intensity ratios of the samples	30
Table 4.2	SE values of the samples.....	33
Table 5.1	EMI SE comparison with other studies	36

List of Abbreviations

GF	Graphene Foam
GF/MnO ₂	Graphene Foam/Manganese Dioxide
GO	Graphene Oxide
rGO	Reduced Graphene Oxide
ZnO	Zinc Oxide
NiO	Nickel Oxide
CNT	Carbon Nanotube
EM	Electromagnetic
EMI	Electromagnetic Interference
SE	Shielding Effectiveness
SE _T	Shielding Total Effectiveness
SE _R	Shielding Reflection Effectiveness
SE _A	Shielding Absorption Effectiveness
RAM	Radar Absorber Material
DoE	Design of Experiment
CVD	Chemical Vapor Deposition
AP-CVD	Atmospheric Pressure Chemical Vapor Deposition

Chapter 1

Introduction

The advancement of electronic information technology brings along some problems caused by electromagnetic (EM) waves. For this reason, electromagnetic absorber materials have recently attracted attention in applications such as electronics, defense stealth technology, and satellite communication systems. These materials provide magnetic and dielectric loss mechanisms that cause interaction with incoming electromagnetic radiation (1). Therefore, EM wave absorber materials should have thin film thickness, lightweight, broad bandwidth, and strong absorption properties for high efficiency (1–3).

Thus, carbon-based nanostructures such as graphene derivatives and carbon nanotubes (CNTs) have become alternative materials since traditional EM wave-absorbing materials cannot meet the demand (4). Graphene and its derivatives can provide the required features for EM wave absorption thanks to their superior properties, such as high thermal conductivity, tensile strength, flexibility, low thermal expansion coefficient, and lightness (5). At this point, using graphene alone may not be sufficient for high microwave absorption (4,6,7).

For this reason, graphene and its derivatives are mainly used with some supporting nanostructures such as ZnO (8–10), MnO₂ (11–13), and NiO (14,15). With this, the obtained hybrid nanomaterials provide enhanced microwave absorption properties by increasing the impedance and interfacial polarization of the structure (4). In addition, graphene-based foams provide a wide range of working areas, especially with their applicable properties (e.g., high surface/volume ratio, interconnected 3D network structure, broadband absorption, and strong desorption) (16). Another purpose of using graphene foam is to create a supportive environment for combining other nanomaterials because of its high synergistic effect (17).

In this thesis study, graphene was synthesized on nickel foam substrate by chemical vapor deposition (CVD) method and then combined with α -MnO₂ nanowire structure using hydrothermal method to measure the EM wave absorption property. It is predicted that combining these two materials increased the EMW absorption performance of the structure. Thus, unlike conventional materials widely studied in microwave frequency technology, graphene in a three-dimensional (3D) foam shape is aimed at increasing the electromagnetic wave absorption capacity. Also, MnO₂ NW increases the GF's surface area and procures enhanced interfacial polarization. In addition, a statistical-based experimental design method was used in this study to save time and cost. In line with the information obtained from previous studies, it is predicted that the GF/ α -MnO₂ nanocomposite structure will be a reference for studies in areas such as intelligent electromagnetic wave manipulation, satellite communication, and radar technologies.

Chapter 2

Electromagnetic Wave Absorption – Materials Interactions

2.1 Electromagnetic Wave Absorption

Microwave and radio wave radiations are spread out by all electronic devices in low frequencies (60 Hz). In free space, EM waves carry energy through photons, and their energy amount affects the wavelength of the EM waves (i.e., lower frequency-lower energy, higher frequency-higher energy). The microwave frequency reference gap is between 3 GHz - 300 GHz, and the electrical wavelength range is between 10 cm and 1 mm, which can be seen in Figure 2.1 (18). When operating the device, the radiated microwaves of electronic devices also cause a frequency penetration or, in other words, EM interference (EMI).

Nowadays, many devices, such as satellites, communication devices, military devices, and other electronic instruments, operate in microwave frequency. Moreover, these microwave frequencies not only cause a malfunction of devices but also affect human health. EMI shielding is the barrier to a radio wave or microwave radiation and prevents interference. Furthermore, the shielding effectiveness (SE) can be tunable with the choice and design of the materials to improve the penetration barrier. With the increasing radiation source and electronics, EMI shielding materials development has rapidly increased over the past two decades (15,19,20).

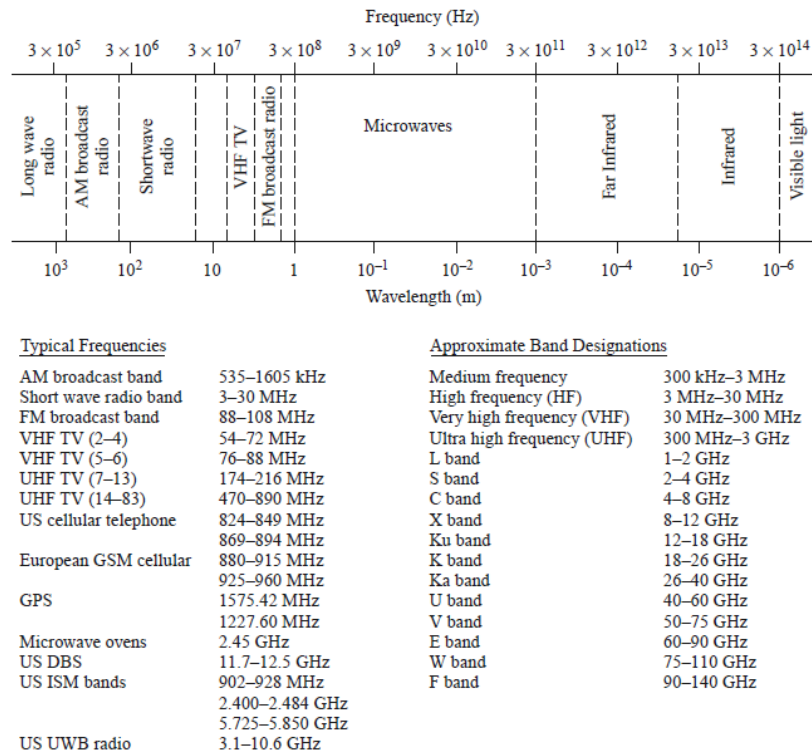


Figure 2.1. The Electromagnetic Spectrum (18)

Absorption and reflection are the main mechanisms of the interaction of EM waves with shielding material. The reflection mechanism takes place on the material's surface as a result of the interaction of charge carriers of material with the EM field, while absorption is a mechanism occurred as a consequence of the interaction of electrical or magnetic dipoles with the radiation. Both mechanisms are dependent on the material's electrical conductivity. Moreover, internal reflection is another interaction mechanism resulting in the absorption of EM waves by scattering the incident radiation at interfaces within the material. Accordingly, absorbed EM waves are turned into thermal energy. On the other hand, materials should reduce the undesired emissions and prevent disoriented external signals for efficient EMI shielding. In addition, absorption is a more crucial mechanism than others that materials should have since reflected waves lead to secondary EM pollution. Therefore, developing absorption-dominant materials is indispensable for high efficiency in preventing secondary EM pollution for many applications (19). Furthermore, an advanced absorbing material should meet the demand, such as lightweight, thinness, low density, absorption ability in a broad bandwidth, corrosion resistance, and electrical conductivity. Together with this, high thermal conductivity is an essential feature for radar-absorbing materials

(RAM) in stealth technology to avoid (e.g., aircraft and drones) from detection by thermal sensors since EM waves are converted into thermal energy (20,21).

Previously, metals and metal particles (e.g., cobalt and iron) had been used as traditional EMI shielding materials. However, metals have become less desirable recently since corrosion tendency and additional weight were considered as drawbacks on military devices in addition to their reflection-dominant EMI SE (5). Therefore, functional materials, such as graphene and its derivatives, have drawn considerable attention to improving effective EMI shielding materials owing to their potential to enable high corrosion resistance, low density, and high strength. Moreover, carbon-based materials offer large-scale production and tunability with other materials and are mostly used as a building block of hybrid structures.

Studies recently concern mainly carbon-based materials as shielding materials because they exhibit splendid EM-absorbing performance due to their high specific surface area and electrical conductivity (22). For instance, Wang et al. synthesized a hybrid structure, reduced graphene oxide (rGO)/ α -Fe₂O₃ nanoparticles, to examine the microwave absorption property. To improve the α -Fe₂O₃ nanostructures' EMW absorption function, rGO was added to the nanostructure. Obtained results show that only α -Fe₂O₃ nanoparticle usage is insufficient for efficient absorption after synthesizing the hybrid structure, and there is a vast difference between the absorption capacity of the α -Fe₂O₃ (RL=-7.8 dB) and rGO/ α -Fe₂O₃ (RL=-38 dB) in the range between 2-16 GHz. Also, it is seen that the increase in thickness and porosity enhanced the EMW absorption (23).

In another study by Pang et al., the effect of carbon nanotubes (CNTs) content and hydrothermal reaction time on EMW absorption performance was investigated. Researchers enhanced the magnetic performance of crystalline manganese iron oxide (MnFe₂O₄) nanoparticles by coated it with CNT. As a result, hybrid structures' reflection loss (RL) reached -38 dB, unlike only nanoparticle absorption measurements (4).

Furthermore, previous studies show that the G/ α -MnO₂ hybrid structure provides an excellent EMW absorption performance in the 2-18 GHz frequency range. Therefore GF/ α -MnO₂ nanostructure is a promising candidate for EMW absorber applications besides energy storage and water oxidation catalysis applications. This thesis study

used CVD-based graphene foam due to its good dielectric loss performance, high specific surface area, and low density. Accordingly, α -MnO₂ nanowires were synthesized on CVD-based graphene foam to enhance the graphene foam's absorption performance by benefiting from MnO₂ nanostructures' interfacial polarization and impedance-matching behavior (24).

2.2 Graphene-Based Electromagnetic Wave Absorbing Materials

EMW absorber materials aim to prevent the spread of undesired EM energy. Reflection, transmission, and absorption phenomena must be pointed out to create effective absorption performance. The absorber materials should scatter or suppress the incident EMW, which is procurable with tunable impedance matching, dielectric loss, and magnetic loss.

Until today ceramics, metals/metal particles, conductive polymers, and their hybrids were leading the absorber materials. Nonetheless, high density, low corrosion resistance, low durability, and insufficient absorption capacity restricted the microwave absorption capacity of these materials. On the other hand, the carbon-based (graphene, carbon nanotube, graphite, carbon black, graphene oxide, etc.) advanced absorber materials have unique features for absorption performance, such as low density, thermal stability, thin film thickness, and wide absorption bandwidth compared with traditional materials (25,26).

In stealth technology, graphene and its derivatives have tunable properties, including production methods (top-down and bottom-up). For example, chemical and synthetic production methods can design complex permittivity, carrier mobility, and electrical conductivity of graphene. Moreover, its well-designed morphology, highly porous, and sandwich-like structure improves the EM interference.

2.2.1 Graphene-Based Magnetic Metal Nanocomposites

Graphene-based magnetic metal composites comprise the hybrid form of magnetic metal particles (e.g., Co, Ni, Fe) and graphene derivatives (e.g., rGO, graphene nanosheet). Through interfacial interaction between graphene's high dielectric behavior and metal particles' magnetic feature, these nanocomposites exhibit excellent EMW absorption capacity (27). Yang et al. synthesized α -Fe₂O₃/3D graphene sponge nanocomposite as an EMW absorber material by template-assisted preparation and co-precipitation. Graphene and metal particles' synergistic effect improved the magnetic/dielectric loss mechanism with enhanced impedance matching. Their results showed tremendous EMW absorption capacity by achieving RL=-55.7 dB at 1.4 mm - 1.7 mm thickness in between 12.30 GHz - 16.72 GHz bandwidth (28). Also, rGO/NiO-based EMW absorber materials have great attention through their easy production methods and high electromagnetic absorption capacity (17). In the study by Zhang et al., they obtained a minimum reflection loss of -55.5 dB at 10.6 GHz with the coating layer 3.5 mm thickness (29).

2.2.2 Graphene-Based Ferrite Nanocomposites

Graphene-based magnetic metal nanocomposites' drawbacks, such as corrosion tendency, limited frequency spectrum capacity, and wide dielectric constant, restrict their potential to be used in the EMI shielding application. In recent years, ferrites have been preferable to combine with graphene because of their high physical and chemical properties and synergistic effect (25). Xu et al. produced a magnetic graphene oxide coated with Fe₃O₄ by an in-situ deposition method. Their results demonstrated that created nanostructure has excellent corrosion resistance and minimum reflection loss of -64.4 dB at 10.8 GHz, which is quite a high value. Furthermore, obtained nanostructure was tested after acid treatment for seventy days, and results still show high electromagnetic wave absorption though 16% decreased magnetization saturation (30). Moreover, Peng et al. obtained high-performance EMI shielding material consisting of rGO and magnetic metal oxide (MnFe₂O₄). Hybrid materials shielding effectiveness of 29 dB at the X band, with an RL of -42.2 dB at 14.1 GHz, was measured. Also, they mentioned that rGO/MnFe₂O₄ composites have easy production

methods and can be used in areas such as MA, EMI shielding, temperature sensing, and electro-thermal deicing (31).

2.2.3 Graphene-Based Polymer Nanocomposites

Above-stated electromagnetic wave absorber materials mentioned are heavy-weight and weak corrosion resistant metal-based nanocomposites. These disadvantages make polymer composites more popular due to their flexibility, lightweight, corrosion resistance, and low-price advantages. Therefore, especially the conductive polymer matrix composites have more attention as an EMW absorber material (3,32). The first use of graphene in the EMI shielding field was rGO/epoxy hybrid structure using the in-situ reduction process. The nanocomposite, which has 15 wt% rGO content, exhibited 21 dB EMI shielding effectiveness in X-band (8.2-12.4 GHz frequency range) and was quite lightweight (33). In the study by Pradhan et al., they produced a polymer composite comprised of pristine graphene, graphene sheets, α -MnO₂ nanorods, δ -MnO₂ nanoparticles, and hydrogenated nitrile butadiene rubber. The obtained composite structure showed improved dielectric, tensile, and EMI shielding features. Therewithal, researchers demonstrated that the tensile strength, dipole moment, and conductivity were increased with increasing graphene addition. Also, the manganese dioxide effect was discussed, and α -MnO₂ nanorods showed better absorption performance due to their high aspect ratio compared to δ -MnO₂ nanoparticles. Furthermore, EMW shielding measurement was achieved at the value of 24.5 dB at a thickness of 2 mm (34).

2.2.4 Graphene-Based Ceramic Nanocomposites

Under extreme conditions like high temperatures, EMW absorber materials must show durability and stability, notably in stealth technology. However, high-performance graphene-based polymer or metal composites may not keep their stability in this kind of severe conditions due to their low chemical bonding structure and low corrosion resistance, respectively. For this reason, the remarkable properties of ceramic materials (zinc oxide, silicon carbide, aluminum oxide, etc.) support EMW absorber materials with their high thermal and chemical stability, high corrosion resistance, and insulator structure. Moreover, owing to ceramics materials' properties, such as microstructure

controllability, electromagnetic capacity, and multi-band absorption, endows to expand absorber materials applicability fields (25,35). Han et al. synthesized rGO/ZnO-hollow spheres nanocomposite by hydrothermal method. The reduced graphene oxide sheets and ZnO nanoparticles' well-matched interaction leads to enhanced dielectric properties with increasing polarization mechanisms and electrical conductivity. The results exhibit that the rGO/ZnO nanocomposite was a great absorber candidate with a measured minimum reflection loss of -45.05 dB at 9.7 GHz, at a thickness of 2.2 mm (8). Another study also focused on the absorber materials' shielding effectiveness at high temperatures. Li et al. worked nanocomposite called on GO/Silicon carbide (SiC) nanowire. In this study, they aimed to increase the low absorption capacity and permittivity of SiC by using graphene oxide, and their results demonstrated minimum reflection loss of the composite was -14 dB at 11.8 GHz with a thickness of 2.7 mm (frequency between 2 GHz and 18 GHz). In addition, they reached these results at a high temperature, which is 1450°C (36). As a result, carbon-based ceramic composite structures show efficient EMW absorption performance in severe conditions (37).

2.2.5 Graphene-Based Multicomponent Nanocomposites

In this section, graphene-based multi-component absorbers' efficiency will be discussed. Graphene-based absorber materials express very effective results; however, supporting the structures' properties with other mechanisms makes graphene-based materials more solid under every condition and field. As mentioned, such properties promote the absorber/shielding effectiveness; therefore, combining two or more material types (e.g., ferrites, ceramics, polymers, metal particles) reveals superior reflection loss and dielectric performance (38,39). So unique properties of three-dimensional structures, such as physicochemical, aroused interest in the EMW absorber field. Consequently, Zhang et al., to benefit from these properties of the graphene-based structures, synthesized 3D cobalt-nickel nanoparticles with nitrogen-doped CNT and reduced graphene oxide sheets (3D CoNi/N-GCNT) together. The nanocomposite's large specific surface area, defects, voids, and abundant interfaces created an excellent absorption mechanism with high mechanical strength and enhanced electrical conductivity (40). Also, Liu et al. worked on multicomponent

hybrid structures, and investigated magnetically decorated G and CuS nanoflakes' (NiFe₂O₄/G/CuS) microwave absorption (MA) properties. The experimental results showed an outstanding MA performance and decreased EM wave irradiation; quantitative results were a minimum reflection loss of -54.5 dB at 11.4 GHz at a thickness of 2.5 mm (41).

2.2.6 Graphene-Based Carbon Material Nanocomposites

Carbon-based materials have drawn much attention due to their superior electromagnetic wave absorption effectiveness properties. In addition, their gifted features, such as low resistivity, conductive features, and polarization loss mechanisms, made them unique in many areas. Moreover, graphene and carbon materials have adjustable defects, dielectric features, corrosion resistivity, and low-weight structure (42). In the study by Chen et al., ultralight multiwalled carbon nanotube (MWCNT)/graphene foam hybrid structure was synthesized via the solvothermal method to examine its microwave absorption effectiveness. The results showed that the hybrid structure exhibits remarkable microwave absorption in low frequencies owing to tunable conductivity and permittivity behavior by regulating MWCNT loading in the structure. Attained reflection loss was -39.5 dB, and absorption intensity exceeded 22.5 dB in both the X band (8-12 GHz) and C band (4-8 GHz) measurements (43). Another group investigated rGO/CNT hybrid's EMW absorption performance by dispersing CNT and rGO into poly(dimethyl siloxane) (PDMS) to achieve high absorption via heterogeneous interfacial polarization. The obtained hybrid structure has a 5 wt% filler load with the 2.75 mm thickness reaching RL= -55 dB at 10.1 GHz. Thereby, Kong et al. showed that the three-dimensional rGO/CNT/PDMS hybrid structure is a great candidate as an EMW absorber material associated with its lightweight and high absorption capacity (44). Like the studies mentioned above, Liu et al. also synthesized ultralight-weight, high-performance EMW absorbing material via the hydrothermal method. They used 3D expanded graphite (EG) and 2D MoS₂ nanosheets to create the 3D network structure. The interconnected porous structure of worm-like graphite enables an enhanced impedance matching with multiple reflections and scatterings of EM waves by means of its natural morphological feature. In addition, to achieve improved dipole and interfacial

polarization, the interfaces were increased via MoS₂ nanosheets. As a result, an efficient EMW absorber hybrid structure via -52.3 dB reflection loss was obtained (45).

Although carbon-based materials have great attention, studies dealing with CVD-based graphene as an EMI shielding material are rare. Nevertheless, the CVD-based graphene structure has a high potential to ensure high EMI SE performance owing to its high-quality originating from its production technique (46). Therefore, more insights are required to utilize the known superior features of graphene in a broad range of applications. Considering this importance, this thesis study is focused on the examined CVD-based graphene foam to combine with MnO₂ nanomaterials as EMI shielding material to guide further studies.

2.3 CVD-Based Graphene Foam and Electromagnetic Wave Absorption

Graphene is an excellent material in the 2D materials world, in favor of its superior properties since it was rediscovered in 2004 by Konstantin Novoselov and Andre Geim using the mechanical exfoliation method from graphite. Graphene is the thinnest and strongest material ever; in addition to that, its lightweight, superhydrophobicity, high electron mobility, and elasticity also make graphene extraordinary (47–50).

Graphene comprises tightly packed monolayer carbon atoms into a two-dimensional (2D) honeycomb lattice. Additionally, it can appear in different allotropes of carbon, e.g., zero-dimensional (0D) fullerenes, one-dimensional (1D) carbon nanotubes, or three-dimensional (3D) graphite. Graphene comprises tightly packed monolayer carbon atoms (C) into a two-dimensional (2D) honeycomb lattice. Carbon atoms have six electrons, separated into two of the inner and four of the outer shell. The outer shell electrons use for chemical bonding, and every carbon atom bond to three carbon atoms on graphene's two-dimensional plane, leaving one electron for electron conduction; it is called pi (π) electrons. These pi electrons enhance graphene's C-C bonds. Moreover, graphene is a zero-gap semiconductor, which provides low resistivity and high conductivity (48). Additionally, it can appear in different allotropes of carbon, e.g., zero-dimensional (0D) fullerenes, one-dimensional (1D) carbon nanotubes, or three-

dimensional (3D) graphite. However, 2D graphene' sp^2 hybridization and atomic thickness (0.345 nm) ensure outstanding properties, such as high electrical-thermal conductivity and mechanical strength (51). The whole of those superior features leads to graphenes becoming the most popular 2D material in many areas, such as supercapacitors (52), EMI shielding materials (53), sensors (54), and solar cells (55).

As far as the author knows there is very limited studies conducted on hybrid structure of CVD-based graphene as EMI shielding material. Chen et al. synthesized CVD-based graphene foam and poly (dimethyl siloxane) (PDMS) composite as an EMI shielding material. This composite exhibited 30 dB EMI shielding effectiveness at a quite low amount of graphene loading conditions, which is relatively high compared with traditional, polymer, or metal-based shielding materials. Moreover, they examined the stability of the hybrid structure by bending the structure 10.000 times, and GF/PDMS hybrid structure showed unique flexibility without damage and loss of shielding effectiveness (56).

Another aspect of this thesis study was the easy production ability of the hybrid structure due to the use of the CVD method to synthesize the graphene foam. The template-assisted CVD method is used most to synthesize 3D graphene foam. In the system, graphene synthesis occurs through carbon precursor, hydrogen, and argon gases flowing into the tube furnace under efficient temperatures. Under these conditions, 2D graphene settle and grows on the metallic or non-metallic template and takes its shape (57).

Also, as a carbon precursor, there are some sources, methane, benzene, polyvinyl-alcohol, and acetylene (used with the flow of argon and hydrogen gases-controlled atmospheres). Furthermore, their utilization temperature ranges between 900°C-1050°C. Experimental processes include several steps to obtain graphene foam by CVD method: cleaning the template, removing the oxide layer on the template (metal substrate), graphene growth (by releasing the carbon source), and metal template etching (after CVD growth of graphene) (35,58).

As a result, large and continuous interconnected surface characteristics of CVD-based graphene foam ensures a high synergistic effect to combine with other nanostructures. Towards the considerations mentioned earlier, remarkable properties of graphene foam provide the required features for EM wave absorbers.

2.4 Electromagnetic Wave Absorption of Manganese Oxide

The microwave loss mechanism is separated into dielectric and magnetic loss. Dielectric loss mechanism can be provided via carbon-based materials, ceramics, and conductive polymers, while magnetic loss can be stabilized by metallic alloys, magnetic/transition metals and their oxides, and ferrites. Besides, reflection loss mechanism is used to measure the EM wave absorption, and -10 dB and lesser dB results exhibit more than 90% absorption of the electromagnetic microwave. To create these mechanisms, some metal oxides (e.g., TiO_2 , MnO_2 , NiO , Fe_3O_4) are valuable due to their easy fabrication, applicability, their low costs, and environmentally friendly nature (59). Especially manganese dioxide (MnO_2) NPs exhibit effective MA performance besides their natural abundance, dielectric performance, easy production methods, non-toxicity, and low cost. Therefore, MnO_2 is a highly attractive metal oxide in many areas, such as EMI shielding, energy storage, and water purification. MnO_2 nanomaterials have different types of structural forms (e.g., α , β , δ , γ), achieving by linking its basic MnO_6 octahedra structure differently. α - MnO_2 differs from the other forms of MnO_6 octahedra owing to its tunnel structure, ensuring changeable cations as desired and providing flexibility (60). Furthermore, several methods, such as hydrothermal, sol-gel, and electrochemical methods, are available to synthesize MnO_2 nanostructures in the required form. Amongst them, the hydrothermal method is one of the most used methods to synthesize MnO_2 nanostructures thanks to its simplest, cost-effectiveness, and ensures the synthesis in low temperatures. Moreover, this method offers an entirely controllable synthesis in terms of time, temperature, and concentration. In addition to these, MnO_2 nanostructures show more preferable compared to the bulk structure of MnO_2 , physicochemical character, higher surface area, and low density. Also, α - MnO_2 exhibits an even larger specific surface area and adsorbs more oxygen to contrast with other morphologic structures (4,61,62). In the study by Wang et al., α - MnO_2 nanowires were synthesized, and the nanowires' lengths were around 30 microns and a diameter of 40 nm, so ultra-long wires were grown via the hydrothermal method. They measured α - MnO_2 NW's MA absorption properties, and the results show that due to its dielectric loss and really high aspect ratio, α - MnO_2 NWs exhibit superior MA absorption properties (63). Song et al. worked on

synthesizing MnO_2 in different crystal structures and morphologies to examine their effects on microwave absorption. As a result of their investigations, in two different phases (α and δ) and two different morphologies (nanowire and microsphere), α - MnO_2 provide better dielectric loss compared to δ - MnO_2 s due to their higher conductivity. When the morphologies were compared, it was observed that nanowires exhibited better absorption properties than microspheres due to having more interfaces and high aspect ratio. The structures compared in the study conducted by Song et al. provide supporting results that electromagnetic wave absorber materials can be synthesized with desired properties by controlling the phase and morphology (64). In the study by Wu et al., MnO_2 layers were synthesized on RGO by hydrothermal method in the EMW absorption field. Similar to the study of Song et al., it has been observed that the electromagnetic wave absorption properties of MnO_2 alone are not sufficient. However, the hybrid structure's minimum reflection loss reached -26.7 dB at 11.04 GHz, at a thickness of 2.6 mm (65). In another study by Zhang et al., GO synthesized in the foam form via the chemical method to obtain a three-dimensional structure, and MnO_2 was grown on GO foam via the hydrothermal method. The most substantial electromagnetic absorption obtained by the final hybrid structure, with a thickness of 2.6 mm, measured at the 7.0 GHz bandwidth with a reflection loss of -53 dB. These study result exhibits the advantages of using graphene in foam form (66).

2.5 Motivation

The literature overview indicates that the GF/ MnO_2 hybrid structure had not been studied in this area compared to other graphene derivatives. In addition, it is noteworthy that mostly GO/rGO was synthesized in foam form by chemical methods as EMI shielding material to resemble the GFs morphology. Another purpose of the favor of CVD-based graphene in the thesis study is to contribute to the electromagnetic absorption property of GF, which is less common in the literature. At the same time, MnO_2 , which is one of the metal oxides with various microstructures, is expected to contribute to the study in the related field thanks to its well thermal stability, supporting nanostructures in different phases and morphologies, easy synthesize and non-toxic behavior. Within the scope of the thesis, it is planned to save time and cost by using appropriate statistical-based experimental design methods. Moreover, it has yet to be encountered in the previous studies, performed experimental design with

GF/ α -MnO₂ nanocomposite used in the EMI shielding, and it demonstrates another aspect of the proposed thesis that will contribute to the literature. Figure 2.2 represents all the experimental steps conducted in this thesis study schematically.

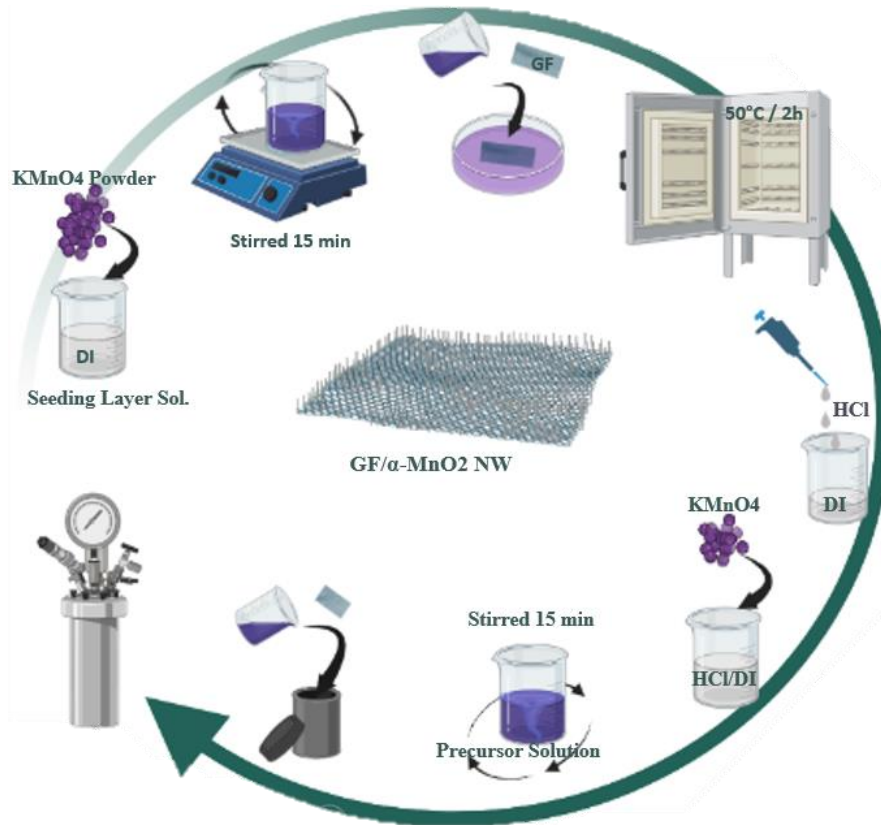


Figure 2.2. GF/ α -MnO₂ hybrid structures experimental steps

Chapter 3

Materials and Method

3.1 Graphene Foam Synthesis via Chemical Vapor Deposition (CVD) Method

Graphene was synthesized on a nickel (Ni) foam substrate (420 g/m² in area density and ~1.6 mm in thickness, Alantum Corp-China) by atmospheric pressure CVD (AP-CVD) under the flow of argon/hydrogen/methane (Ar/H₂/CH₄) (1000/10/20 sccm) gases at 1000°C. All gases were at high purity. Before synthesizing the graphene, Ni foam was cleansed with acetone to prevent contaminations. After the cleaned Ni foam was placed into the tube furnace, before releasing the CH₄ also, its surface oxide was removed via H₂ and Ar gases. The synthesized Ni-G structure was then coated with poly (methyl methacrylate) (PMMA, Mw~996000, Sigma-Aldrich) and cured at elevated temperatures for 15 min. Later on, to eliminate the nickel from the PMMA-coated graphene, the Ni-G/PMMA was immersed in 3M HCl acid (HCl, 37%, Sigma-Aldrich) solution for 5 hours at 80°C. Next, the obtained G/PMMA structure was washed with distilled water and placed into hot acetone (C₃H₆O, purity ≥99.5%, Sigma-Aldrich) to remove the polymer residual. Finally, bare graphene foam was washed with DI and dried.

3.2 Seeding Layer Application of Graphene Foam

The seeding layer was applied on the graphene foam surface to create nucleation sites for the growth of MnO₂ nanostructures and stabilize the propagation. The seeding layer concentration was decided via a preliminary experimental study. First of all, four

different concentrations of potassium permanganate (KMnO_4 , purity $\geq 99.0\%$, $M_w=158.03$, Isolab) aqueous solution was prepared; 0.025 M, 0.050 M, 0.075 M, and 0.1 M. Then graphene foams were immersed into seeding layer solution for 15 min at room temperature and dried for 2 hours at 50°C . Among the seeding layer solution concentrations, synthesized GF/ MnO_2 NWs with 0.075M concentration characterizations resulted in better NW content and regularity. Therefore, hydrothermal synthesis was maintained with a 0.075 M concentration of $\text{KMnO}_4/\text{H}_2\text{O}$ formulation to obtain GF/ α - MnO_2 NWs.

3.3 Experimental Design

Design of Experiment (DoE) is an approach involving several statistical methods to obtain a systematic roadmap for experiments and manufacturing processes by correlating pre-defined design variables. Accordingly, it is crucial to determine the most proper method among DoE methods, such as Full Factorial, Central Composite, Box-Behnken, and Taguchi, according to the relevant experimental conditions to interpret the phenomenon realistically (67,68). Among these, the full factorial design constitutes the experimental runs by associating factors with every other one, so all possible combinations of design variables are considered (67).

Within the scope of this study, a full factorial design was performed by Design-Expert software to build a dataset for further studies alongside generating a systematic roadmap. The reason behind choosing the full factorial design in this thesis is to evaluate all possible matching of parameters with each other. With this intent, temperature, time, and solution concentration were determined as factors to be used in the full factorial design to investigate the effect of hydrothermal process parameters on the EMI SE of GF/ MnO_2 nanocomposite. Based on the literature studies, the factor levels were specified in an interval as a minimum and maximum value by targeting to synthesize MnO_2 in nanowire form due to its high surface area and EM wave absorption capability (64,69–73). Table 3.1 shows factors with their levels used in the full factorial design.

Table 3.1. Variables utilized in full factorial design with their levels

Factors	Levels	
	min.	max.
Temperature (°C)	140	180
Time (h)	6	12
Concentration (M)	0.07	0.2

3.4 Graphene Foam/ α -MnO₂ NWs Synthesis via Hydrothermal Method

The seed-induced GF samples followed the hydrothermal process for α -MnO₂ NWs synthesis. First, the hydrothermal route's precursor solution concentration was defined via experimental design. After that, achieved literature survey parameters were performed by the Design-Expert, and obtained possible combinations were used for the experimental section.

Table 3.2. Experimental design results

	Factor 1	Factor 2	Factor 3	
Run	Temperature (°C)	Time (h)	Concentration (M)	pH
F-1	140	6	0.07 M	0.93
F-2	180	6	0.07 M	0.96
F-3	140	12	0.07 M	0.95
F-4	180	12	0.07 M	0.95
F-5	140	6	0.2 M	1.54
F-6	180	6	0.2 M	1.45
F-7	140	12	0.2 M	1.45
F-8	180	12	0.2 M	1.30

For the first four samples of hydrothermal synthesis, the precursor solution (0.07 M) consists of 0.1 M KMnO₄ powder and an aqueous 0.15 M HCl solution. This solution was stirred for 10 min, then seed-induced graphene foams and precursor solution were

transferred into a 100 ml Teflon-lined stainless-steel reactor. Next, for the α -MnO₂ NW synthesis, the reactor was placed into an oven at the listed temperature and times demonstrated in Table 3.2. Samples named F-5, F-6, F-7, and F-8 were then synthesized by parameters shown in Table 3.2, and the precursor solutions were comprised of 0.008 M KMnO₄ and an aqueous 0.04 M HCl solution.

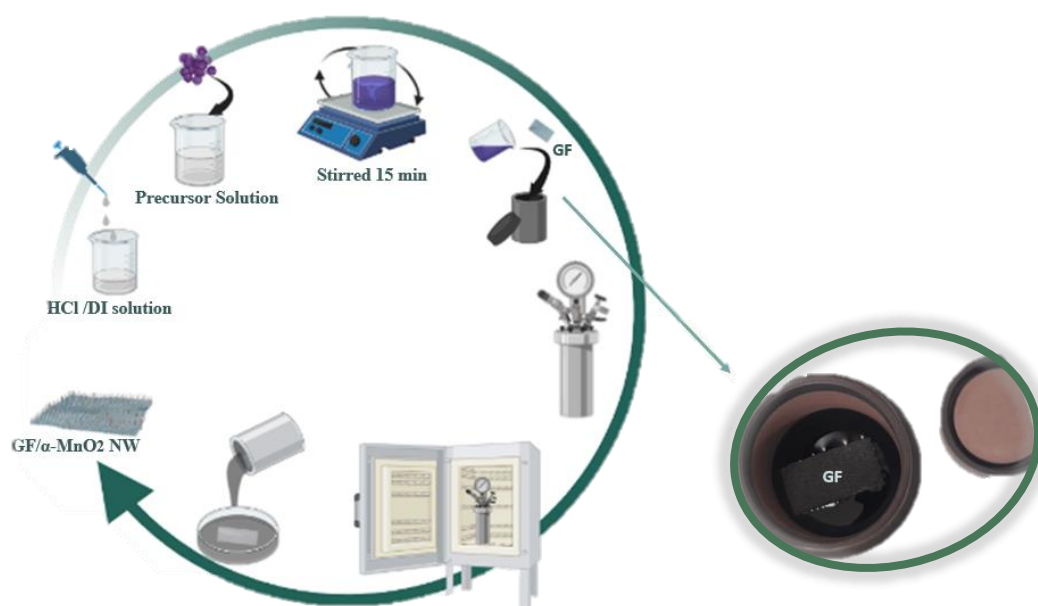


Figure 3.1. Graphical abstract of the MnO₂ NW growth via hydrothermal method

3.5 Characterization

The GF/ α -MnO₂ NWs morphological investigation scanning electron microscopy (SEM, Carl Zeiss Sigma, 300 VP) was performed. The magnifications of the samples were x100, x5.00k, and x10k. Additionally, X-ray diffraction (XRD, Siemens D-500 diffractometer, Thermo Scientific ARL) detected each sample's phase composition with Cu-K α radiation ($\lambda = 0.15418$ nm). XRD analysis was performed in the range between $10^\circ < 2\theta < 70^\circ$ with the $2^\circ/\text{min}$ scanning speed. Raman spectroscopy (Renishaw/inVia™ confocal Raman microscope) was utilized for structural characterization using a 532 nm wavelength laser. EMI SE of GF/ α -MnO₂ NWs hybrid structures was measured in 8-12 GHz bandwidth (X-band) through a two-port vector network analyzer (VNA, Agilent Technologies N5230C, DEU/EMUM). The achieved

scattering parameters (S-parameters), denoting the input-output relationship of a network with N ports, were converted to the relevant shielding effectiveness (SE) values of hybrid structures by the following equations showing the interconnection of total SE with absorption, reflection, and multiple internal reflection mechanisms (74):

$$SE_T = 10 \log_{10}(1/|S_{21}|^2) \quad (1.1)$$

$$SE_R = 10 \log_{10}(1/(1 - |S_{11}|^2)) \quad (1.2)$$

$$SE_T = SE_A + SE_R + SE_M \quad (1.3)$$

where SE_T , SE_R , SE_A , and SE_M correspond to shielding effectiveness originating from total, reflection, absorption, and multiple internal reflection loss, respectively. In equations (1.1) and (1.2), $|S_{11}|^2$ and $|S_{21}|^2$ are S-parameters representing the reflection and transmission coefficients obtained from VNA, respectively. It should be emphasized that both transmission and reflection coefficients should be considered as fractions or percentages rather than in dB unit (74). Moreover, the SE_M mechanism is assumed negligible when total effectiveness is over 15 dB. Hence, equation (1.3) can be written for SE_T , and SE_A can be derived in terms of S-parameters as follows (74,75):

$$SE_T = SE_A + SE_R \quad (\text{when } SE_T > 15 \text{ dB}) \quad (1.4)$$

$$SE_A = 10 \log_{10} ((1 - |S_{11}|^2)/|S_{21}|^2) \quad (1.5)$$

Chapter 4

Result and Discussion

4.1 Scanning Electron Microscopy (SEM)

The GF/MnO₂ hybrid structures' morphological characteristics were examined along with the SEM images. Considering the SEM images, only two samples were fully covered with MnO₂ NWs. Therefore, the literature-based synthesis parameters deficiencies emerged with this thesis's experimental results. According to the synthesis parameters design with upper and lower limits, the intermediate values also must be in the experimental design to reach the most effective results in the study. Figure 4.1 showed that x100 magnification of the samples, the first image (a) indicates the bare graphene foam; the 3D structure and regular shape of the graphene foam were preserved well, even after some chemical treatments, as mentioned in the graphene foam synthesis section. The rest of the images indicate F-1, F-2, F-3, F-4, F-5, F-6, F-7, and F-8 respectively. Figure 4.1, images c (F-2), d (F-3), and e (F-4) express the damaged foam morphology due to the hydrothermal parameters used (temperature, concentration, and time). Thus, it is thought that for the growth of MnO₂ nanostructures, high temperatures (180°C) and too-low pH values were not eligible. These growth parameters were also damaged to the graphene architecture, as seen more closely in Figure 4.1, which shows the x1.00k magnification of samples. Besides, Figure 4.1 demonstrates only GF/MnO₂ hybrid structures. Here, it can be seen that Figure 4.1, e, and g have much more nanowires on the graphene foam with some agglomerations. As compared F-5 (e) to F-7 (g) samples, results showed nanowire diameter and agglomerations were increased via increased synthesis temperature and time parameters. Due to the high supersaturation degree, the diffusion mechanisms break at high temperatures, and aggregations will occur. However, it leads to thick and

rough nanostructure growth. Figure 4.1, e (F-5) has a fine MnO₂ nanowire structure due to the low synthesis temperature and relatively high pH value of precursor solution concentration compared with Figure 4.1, g (F-7). Moreover, it is proved with the sample named F-8 (Figure 4.3, h) the high temperature and time parameters tend to cause an overgrowth of nanowires' diameters and agglomerations. Therefore, all synthesized samples demonstrated that the experimental process parameters must be at lower temperatures and time together with efficient solutions concentration.

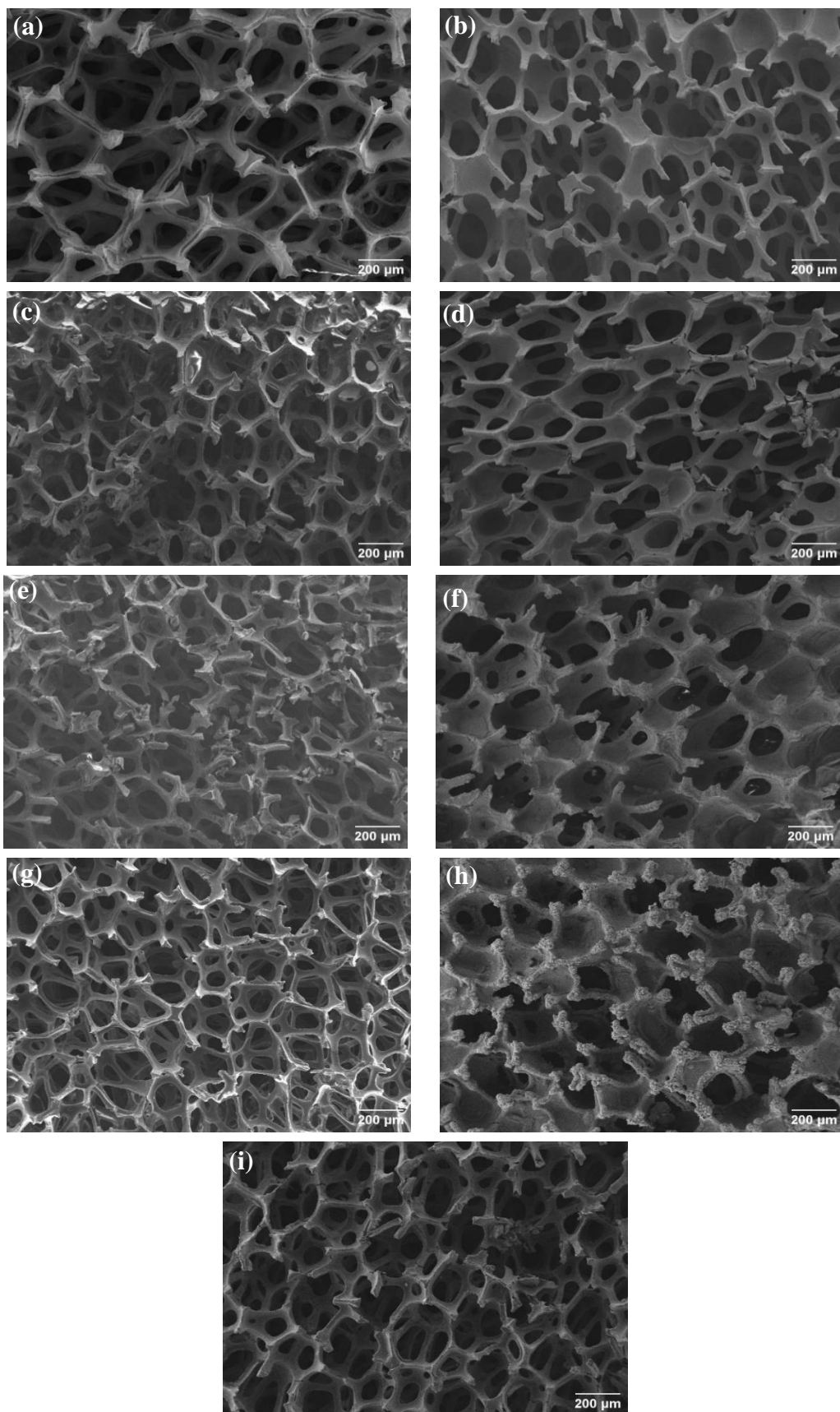


Figure 4.1. x100 SEM images, GF, F-1, F-2, F-3, F-4, F-5, F-6, F-7, F-8 respectively

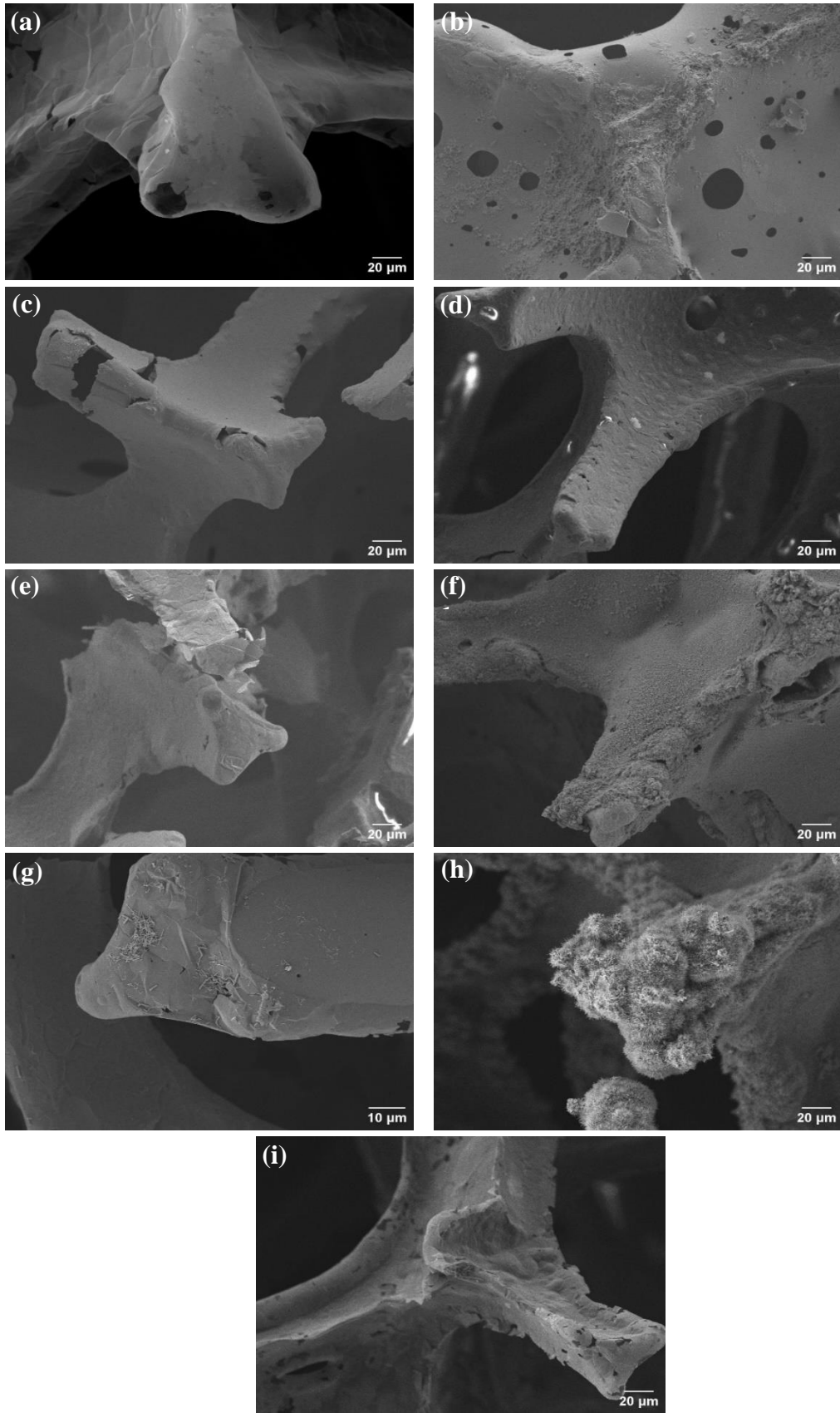


Figure 4.2. x1.00k SEM images, GF, F-1, F-2, F-3, F-4, F-5, F-6, F-7, F-8 respectively

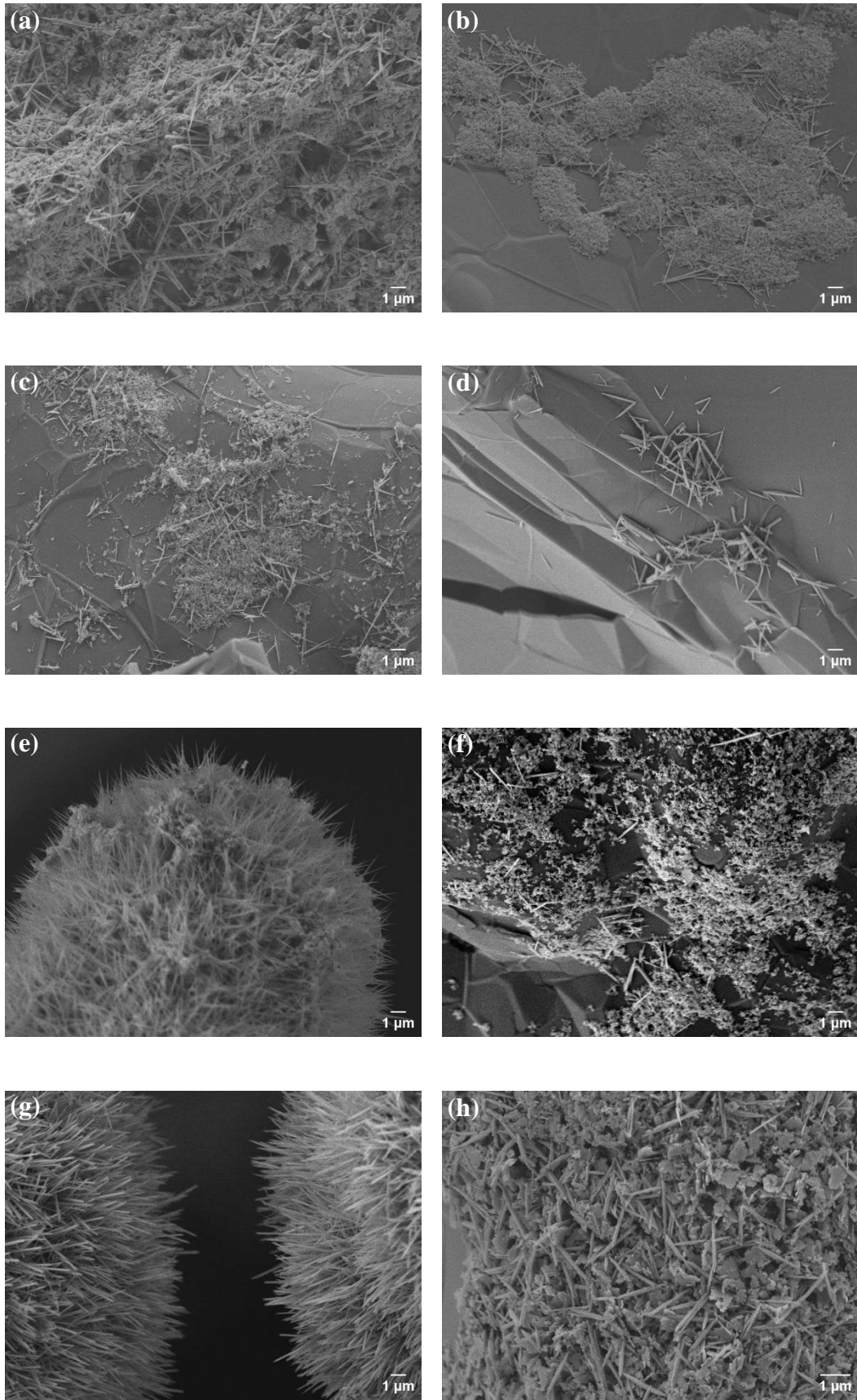


Figure 4.3. x10.00k SEM images, F-1, F-2, F-3, F-4, F-5, F-6, F-7, F-8 respectively

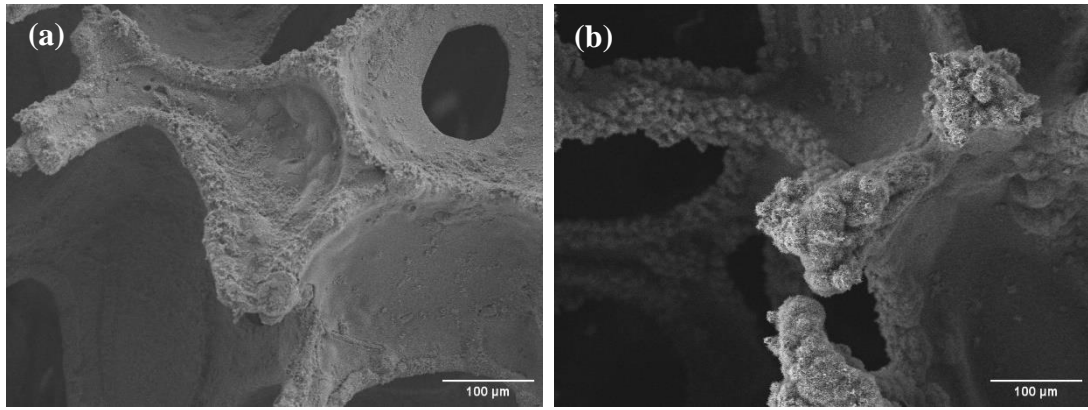


Figure 4.4. x500 SEM images of F-5 and F-7 respectively

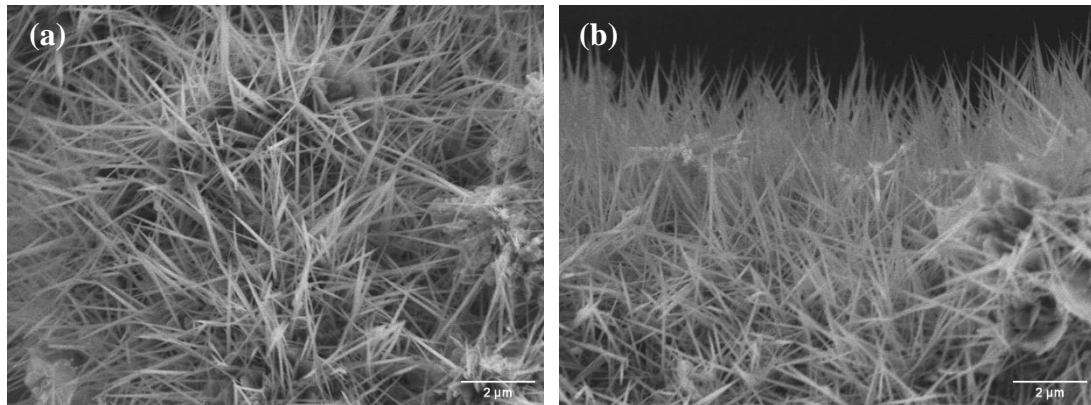


Figure 4.5. x20.00k SEM images of F-5 and F-7 respectively

4.2 X-Ray Diffraction Analysis (XRD)

The XRD graph of the GF/MnO₂ nanocomposites accomplished to examine the changes in the crystallographic structure depending on the hydrothermal solution concentration, time, and temperature are shown in Figure 4.5. The spectra indicate that α -MnO₂ NWs and GF peaks were obtained successfully. Figure 4.4 shows the XRD pattern of GF/ α -MnO₂ NWs and GF, which correspond to the standard cards for α -MnO₂ and carbon, JCPDS 44-0141 and JCPDS 75-1621, respectively. This figure shows the XRD pattern of the α -MnO₂ NWs with nine well-defined diffraction peaks with 2θ values of 12.98°, 18.34°, 28.78°, 37.66°, 42.14°, 49.90°, 56.44°, 60.26° and 65.84°, correspond to the (110), (200), (310), (211), (301), (411), (600), (521), and (002) respectively, reflecting α -MnO₂ tetragonal phases (JPCDS44–0141).

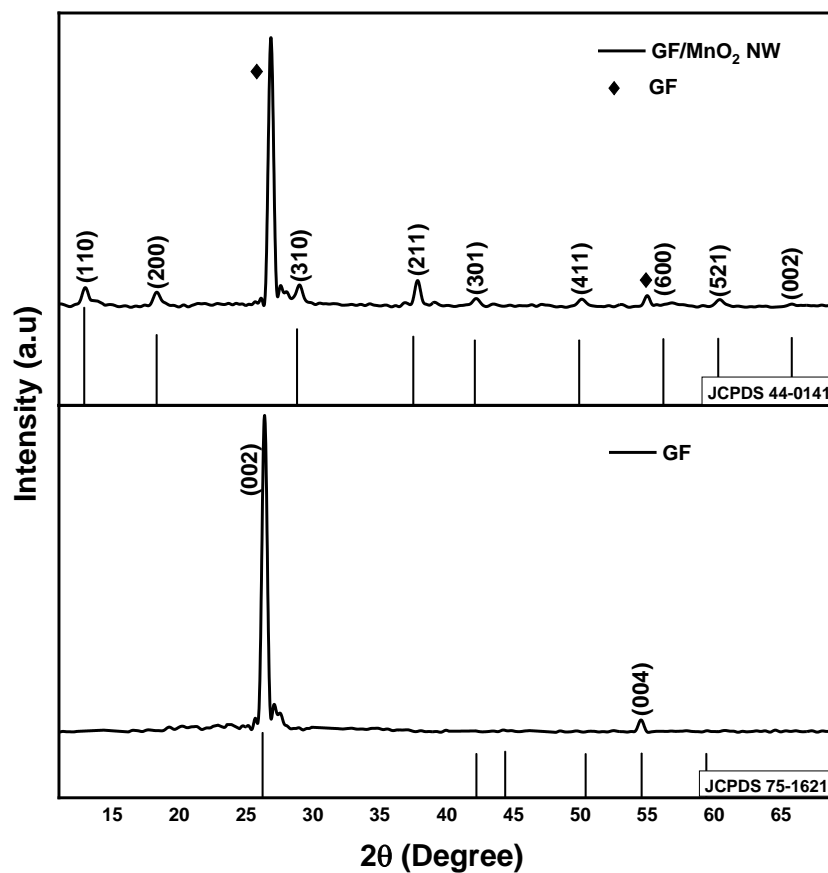


Figure 4.4. XRD graph of the GF and GF/ α -MnO₂

Furthermore, according to JCPDS 75-1621, the XRD spectrum of GF's corresponds to the two prominent peaks $2\theta=26.2^\circ$ and 54.5° (002) and (004) of the graphene structure. This observation is the clearest evidence that nanocomposite components are present in GF and MnO₂ NW in perfect harmony and high purity without damaging the crystal structure. Nevertheless, the SEM images demonstrate that not all samples are fully covered with MnO₂ NWs except F-5 and F-7. At this point, we can say that the MnO₂ NWs in the alpha phase show more regular and intense growth on GF by increasing the amount of KMnO₄ and synthesizing them at low temperatures.

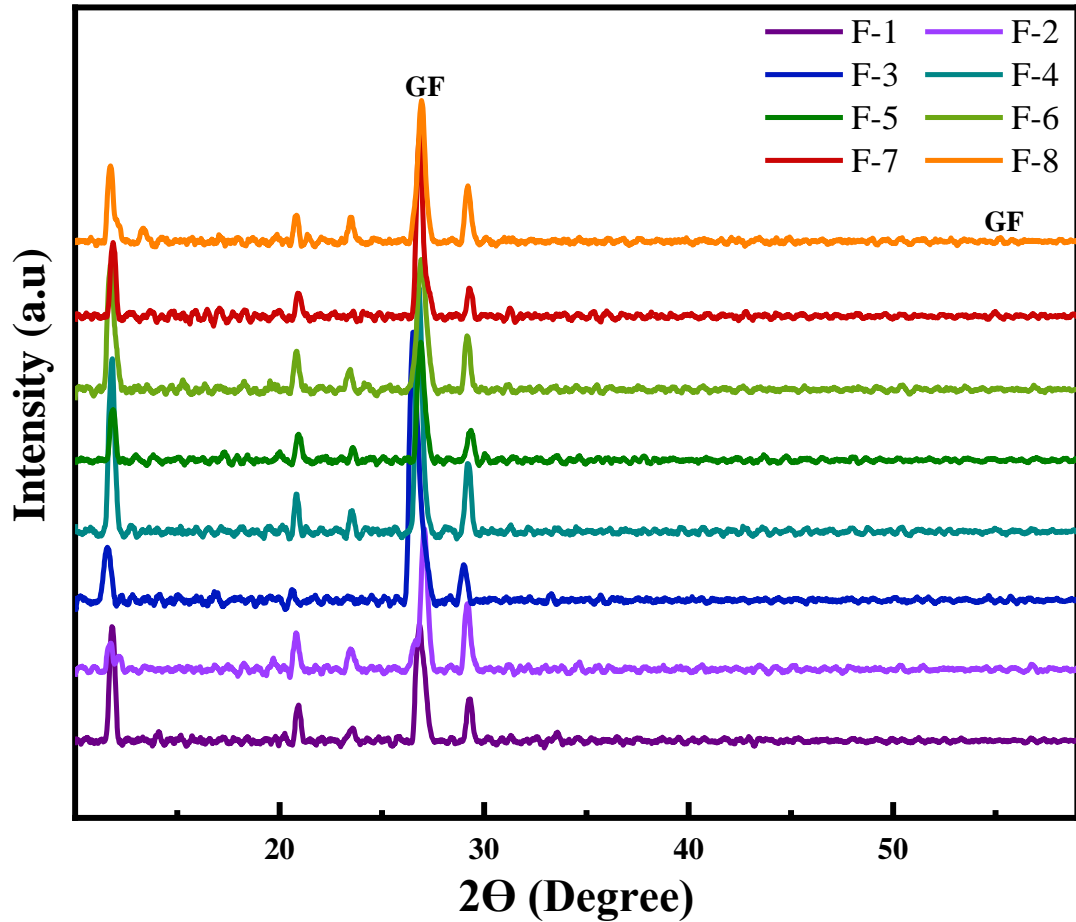


Figure 4.5. XRD graph of the all GF/ α -MnO₂ samples

4.3 Raman Spectroscopy

The Raman spectroscopy of the samples in Figure 4.6 shows that the four characteristic peaks 180, 356, 576, and 640 cm^{-1} are associated with Mn-O lattice vibrations in α -MnO₂ and Mn-O-Mn bending modes. Previous studies have supported the presence of a strong peak of about 640 cm^{-1} and weak bands of about 180, 356, and 576 cm^{-1} (76,77). Furthermore, prominent Raman peaks in graphene were observed around 1350, 1580, and 2697 cm^{-1} , corresponding to D, G, and 2D bands. Thus, GF and α -MnO₂ nanostructures are utterly present in the structure, as mentioned in the XRD analysis results.

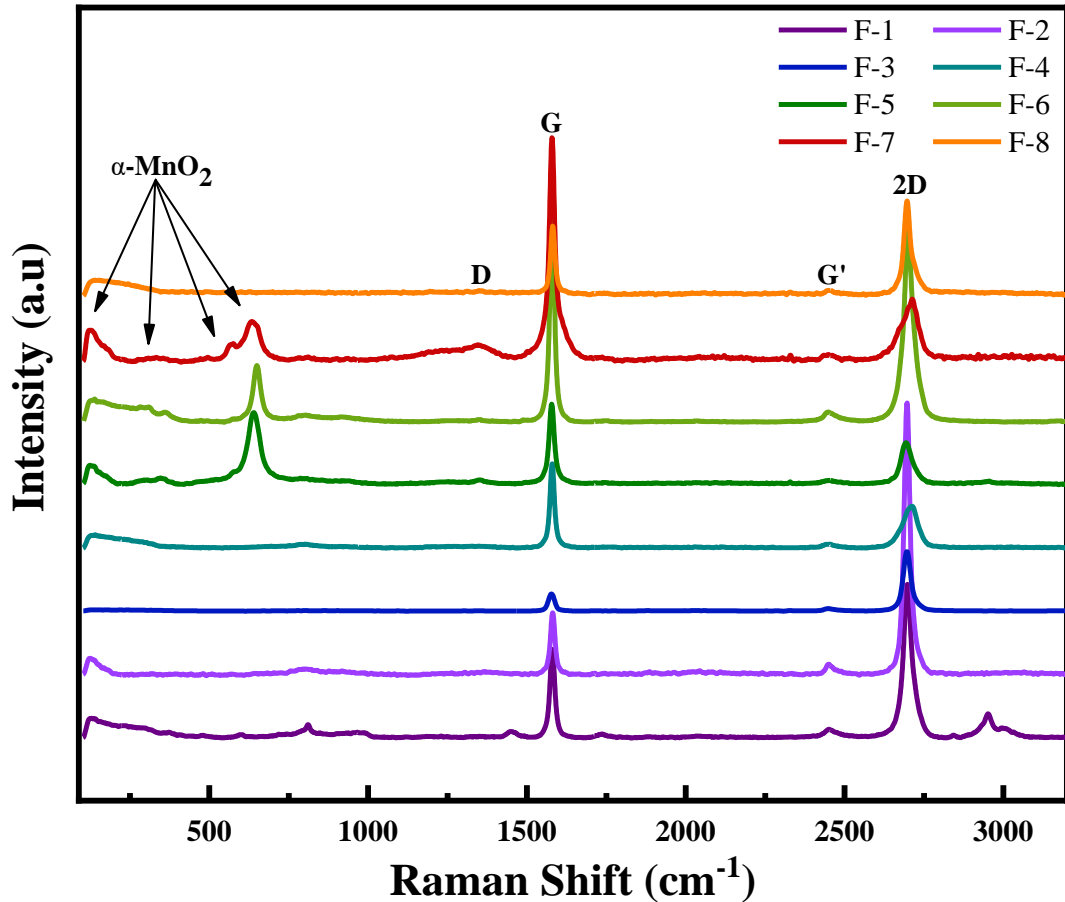


Figure 4.6. Raman spectrum of the GF/ α -MnO₂ samples

D band indicates the structural defects, and the G band reveals the crystallinity of the graphene. The intensities ratios of these bands (I_D/I_G) allow us to determine the structural disorder of the graphene (78). Besides, the intensity ratios of the 2D and G bands (I_{2D}/I_G) display the graphene layer numbers; Table 4.1 demonstrates these intensity ratios. Sample F-1 has the lowest I_D/I_G ratio (0.02), while F-3 has the highest ratio (0.88). As a consequence of the ratios, there are several outputs; the graphene foams have a large specific surface area and high electron mobility, providing an active surface for the growth of the MnO₂ nanostructures. Also, their synergistic harmony ensures a fast and reversible redox reaction on the surface of the graphene. In addition to that, the increased nanostructure concentration on the graphene surface leads to changes in crystallinity owing to carbon atoms reduction (13,51). These reasons and GF's natural defect feature affect the peak intensities ratio. Considering the I_{2D}/I_G ratios of the samples, Table 4.1 demonstrates that F-1 and F-2 samples were single layers, and the rest were bilayer graphene. However, graphene foam structures' layer number

variability also displays their structural irregularities (79). Additionally, the 2D bands' rightward shifting expresses the mechanical strain among the GF and MnO₂ atoms via the decreased phonon energy (80).

Table 4.1. Raman spectrum intensity ratios of the samples

Sample	I _D /I _G	I _{2D} /I _G
F-1	0,02	1,7
F-2	0,52	2,7
F-3	0,88	1,3
F-4	0,7	0,9
F-5	0,77	0,9
F-6	0,6	1,0
F-7	0,66	0,7
F-8	0,87	1,1

4.4 Vector Network Analysis (VNA)

There are three mechanisms of EMI SE consist of absorption (SE_A), reflection (SE_R), and multiple reflections (SE_M), and multiple reflections are negligible when SE (Total) is more than 15 dB. Therefore, SE_A, SE_R, and SE_T graphs are given in this section. The SE absorption mechanism interacts with the electromagnetic waves and converts EM energy to internal/thermal energy. Moreover, the reflection mechanism works with the conduction of the charge carriers; mostly, conductive materials exhibit high reflection. Therefore, these two mechanisms (SE_A and SE_R) dominate the EMI SE. As concerns, EMI SE demonstrates the percentage of blocked waves by the material. In general, greater than 20 dB EMI SE value indicates the incident radiation blocked 99% (81).

The Figure 4.7 represents the result of the maximum SE_T values of hybrid structures: F-7>F-5>F-2>F-1>F-3>F-6>F-8>GF≥F-4. As expected, the highest two SE_T values belong to samples F-7 (53 dB) and F-5 (36 dB) due to their MnO₂ NWs content. The sample's foam structure may be damaged by reason of sample preparation and the way to place it on to VNA waveguide. Therefore, the difference between the samples may be caused by defects or damage.

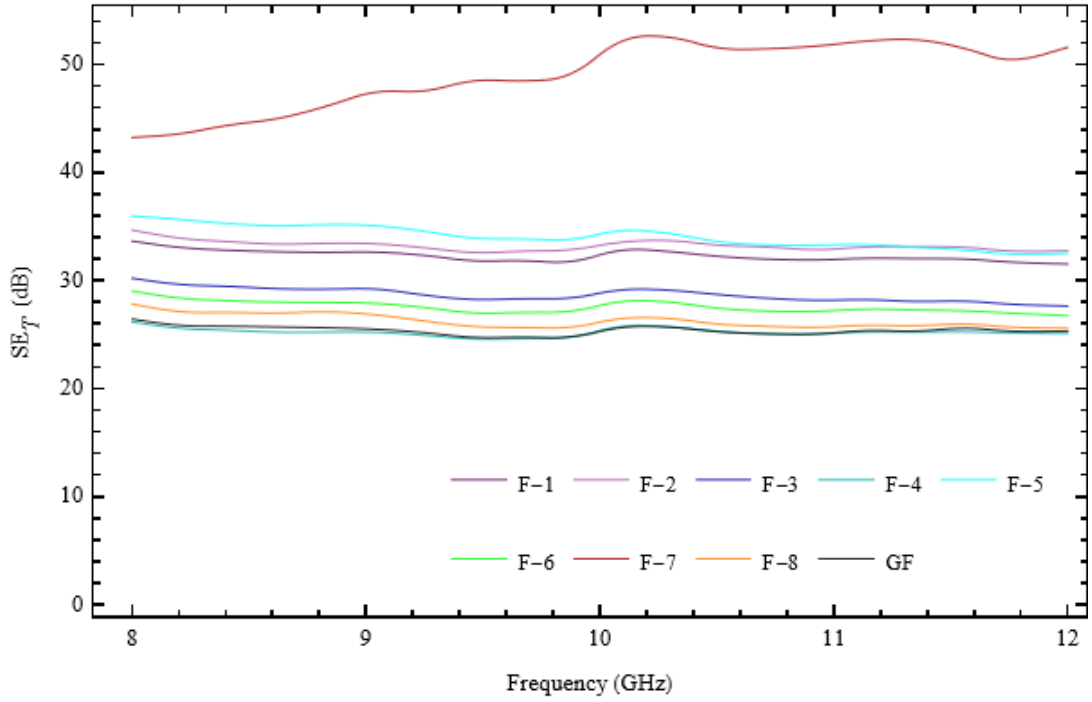


Figure 4.7. SE Total of all GF/MnO₂ samples

Besides the total shielding effectiveness, the absorption and reflection capacity of the samples is essential; Figure 4.8 (SE_A) indicates the absorption effectiveness values, and the order from highest to lowest value is as follows; F-7>F-5>F-2>F-1>F-3>F-6>F-8>F-4>GF, which are very similar to the order of the SE_T results. Considering Figure 4.9 (SE_R), values of the reflection effectiveness are as follows; GF>F-1>F-2>F-6>F-3>F-4>F-8>F-5>F-7. As a result, GF/MnO₂ hybrids named F-7 and F-5 exhibited great shielding effectiveness by supporting the structure via excellent absorption and minimum reflection capacity.

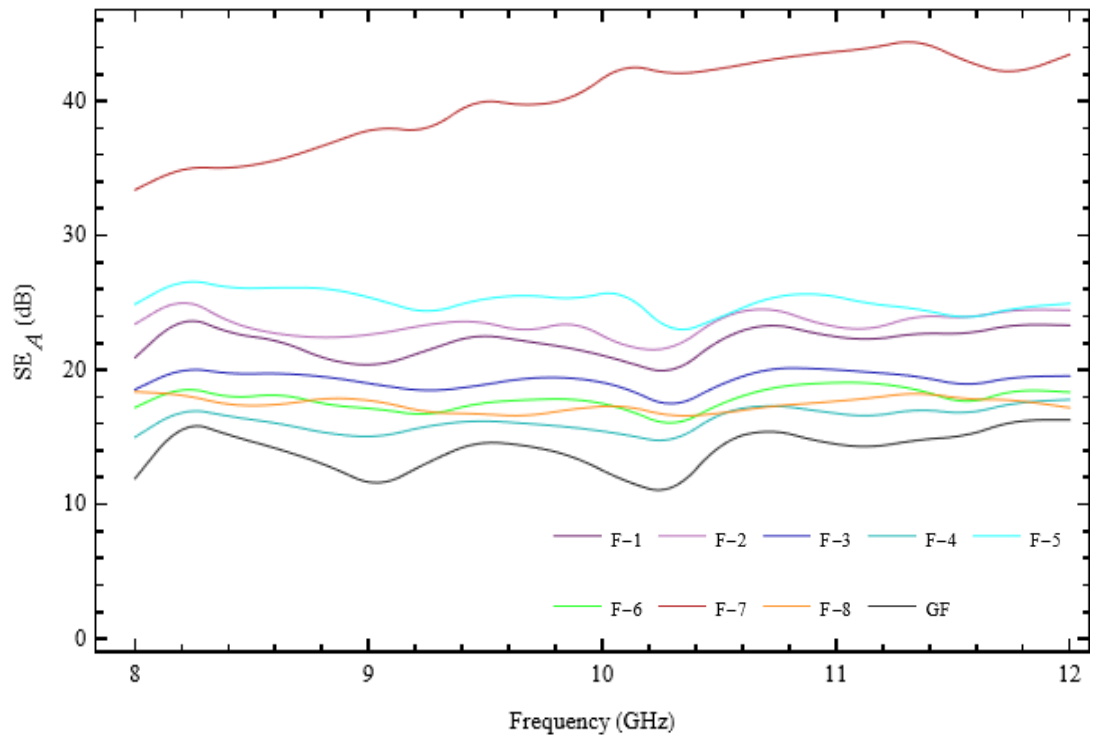


Figure 4.8. SE Absorption of all GF/MnO₂ samples

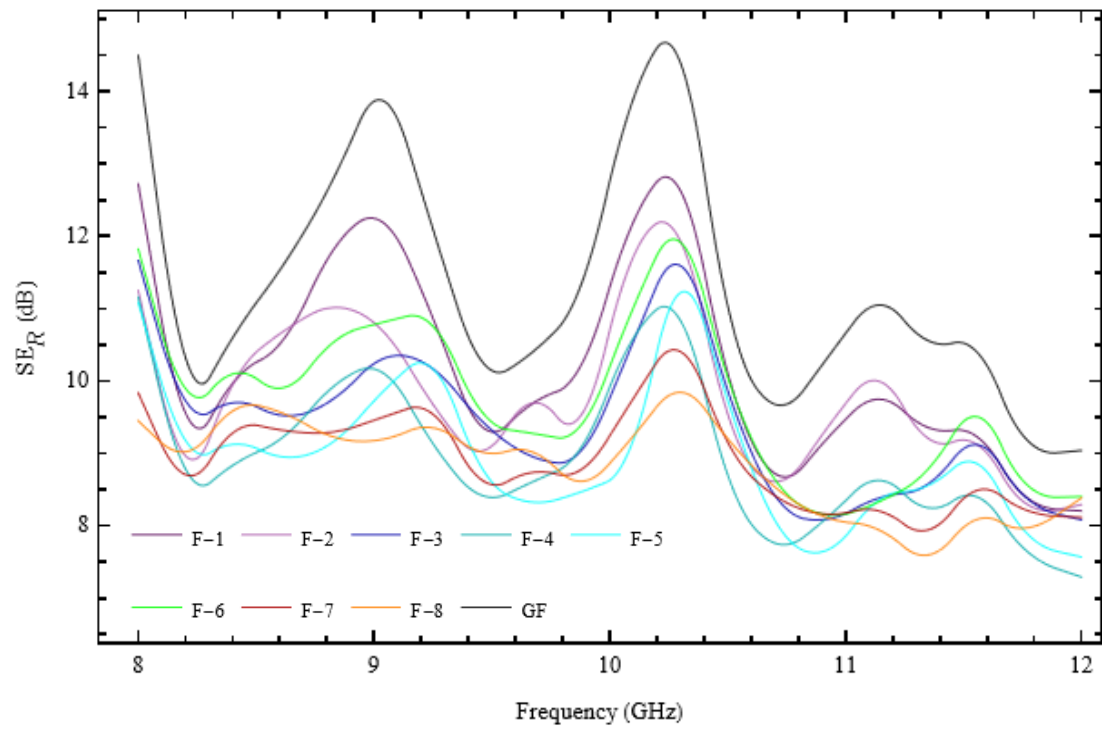


Figure 4.9. SE Reflection of all GF/MnO₂ samples

Table 4.2 expresses the sample's total shielding effectiveness values with their absorption and reflection ranges. With this table, the exact absorption and reflection measurements are clearly seen. The observed results of the samples GF and F-4 also proved that total SE values were essential; however, the reflection and absorption ratios must be controlled to detect the exact shielding effectiveness mechanism of the final structure. The absorption-dominant shielding performance was achieved except for the GF sample, even with wire content deficiency for all GF/ α -MnO₂ hybrids. Consequently, for EMI shielding materials, it can be said that if graphene is supported via additional nanostructure, the reflection-dominant mechanism can be changed to an absorption-dominant mechanism.

Table 4.2. SE values of the samples

Sample	SE _T (dB)	SE _A (dB)		SE _R (dB)	
		max	min	max	Min
GF	26.41	16.52	6.70	18.70	8.71
F-1	33.64	23.97	17.24	15.32	7.95
F-2	34.66	25.37	19.35	13.64	7.94
F-3	30.20	20.94	17.33	12.54	7.48
F-4	26.15	17.79	13.73	11.63	7.22
F-5	35.97	27.25	23.12	11.93	7.21
F-6	29	19.64	15.35	12.63	7.57
F-7	52.79	44.99	33.39	11.25	7.35
F-8	27.82	19.37	15.32	11.01	7.31

Chapter 5

Conclusion

EMI shielding materials draw great attention, especially in stealth technology. In recent years, carbon-based EMI shielding materials demonstrated high shielding effectiveness with an enhanced absorption capacity. Nevertheless, almost all designed carbon-based absorber materials are synthesized using GO and CNT. To benefit from the foam structures' interconnected network structure and large, porous surface area, the researchers have been synthesizing these carbon-based materials in foam shape using chemical methods. One of the distinguishing aspects of this thesis is the use of CVD-based graphene foam; compared to GO and CNT, there are very limited study dealing with CVD-based graphene as an EMI shielding material. Nevertheless, the CVD-based graphene structure has a high potential to ensure high EMI SE performance owing to its high-quality originating from its production technique. However, combining two or more material types (e.g., ferrites, ceramics, polymers, metal particles) with graphene, reveals superior reflection loss and dielectric performance.

This thesis presented a successfully synthesized CVD-based GF/ α -MnO₂ NW hybrid structures as an EMI shielding material. Before starting the laboratory experiments to obtain desired nanostructures, the experimental design was performed to achieve a systematic roadmap. The design parameters included the hydrothermal process parameters such as temperature, time, and precursor solution concentration. Based on the literature studies, factor levels were specified in an interval as a minimum and maximum value by aiming to synthesize MnO₂ in nanowire form due to its high surface area and EM wave absorption capability. Then, obtained design parameters were used for the growth of MnO₂ NW by hydrothermal synthesis.

After experimental studies, the critical parameters were well understood in the MnO₂ NW growth mechanism. Obtained GF/ α -MnO₂ hybrid structures' SEM images indicate several morphological tendencies of the MnO₂ nanowire growth mechanisms.

- Concerning preliminary studies, results show that the seeding layer application dominates the morphological changes of the MnO₂.
- Precursor solutions that were saturated per K ions provided an increase in MnO₂ NW length.
- The thickness of the nanostructures was increased with increasing synthesis temperatures.
- High synthesis temperatures were nonviable for the growth of MnO₂ nanostructure due to the high supersaturation levels hindering the nanostructures' agglomerate and growth.
- Lower pH values (below 1.0), while damaging the graphenes' foam structure, prevented the nucleation propagation of the MnO₆ octahedra.
- Long periods of reaction times ensure the refinement of the MnO₂ nanowire morphology.

Experimental results show that the CVD-based graphene foam's absorption performance was not as high as their hybrids; even so, the EMI SE performance of GF was measured as 26 dB with more than 99% effectiveness. On the other hand, GF/ α -MnO₂ hybrid structure exhibits superior EMI SE, which is more than 99.999% (81) with 53 dB at a frequency range of 8-12 GHz. As a result, this study demonstrated the GF/ α -MnO₂ NW hybrid structure as a promising candidate as an EMI shielding material. Considering the excellent EMI SE measurements, this hybrid structure can be used as well for commercial applications such as stealth technology and guide further studies.

Outlook and Future Works: The absorption-dominant EMI shielding mechanism is crucial for EMI shielding materials; with this mechanism, the secondary EM pollution created by reflected EM waves can be controlled and decreased. With this aim, the chosen materials must be in harmony with each other and show high absorption behavior. In this study, the GF/ α -MnO₂ hybrid material provides unique absorption by comparison with the other carbon and traditional EMW absorber materials. By using

CVD-based graphene foam, we acquired a well-designed morphology, highly porous 3D structure, high thermal and electrical conductivity, and lower density design. Additionally, α -MnO₂ nanowires were grown on the graphene foam to support and enhance the absorption performance. The α -MnO₂ NW's dielectric and magnetic loss mechanisms increase the MA performance of the hybrid structure. Also, their non-toxicity, natural abundance, and easy production methods make them preferable. In the preferred design, while the MnO₂ nanostructure was used in wire form, the G was used in foam form; with this hybrid structure, we achieved morphological advantages of creating more surface area and internal reflections to dissipate the EM waves by using the structural benefit of the nanowires and 3D GF structure.

Table 5.1. EMI SE comparison with other studies

Materials	Thickness (mm)	EMI SE (dB)	Frequency Range	Ref.
Graphite oxide/Epoxy	-	21	X-band	(33)
GnP/ α -MnO ₂ / δ -MnO ₂ /HNBR	2	24.5	X-band	(34)
MWCNT/GO foam	2	22.5	X-band	(43)
GF/PDMS	~1	30	X-band	(56)
PDA/rGO foam	~0.032	26.5	X-band	(82)
GF/ α -MnO ₂	~1.5	53	X-band	<i>This study</i>

In order to optimize the GF/ α -MnO₂ NW hybrid structure, many options can be considered; for instance, each additional ferrite, polymer, ceramic, or metal particle will reveal a different shielding mechanism improvement. Especially in the preferred design (GF/ α -MnO₂), adding polymer as a matrix material will increase the reflection loss much more than in Chen et al.'s (56) study due to the escalated interfacial polarization via MnO₂ NWs.

Compared with the other studies, the GF/ α -MnO₂ hybrid structure's EMI SE value is quite high. PDMS may be used for further studies to preserve the foam structure and give extra flexibility. Also, the polymer's high corrosion resistance, lightweight, and low-price advantages provide high applicability for EMI shielding materials. Besides, highly magnetic metal oxides can be added to the structure to achieve enhanced impedance matching and loss mechanisms.

Lastly, the experimental design used in the study should be repeated by adding intermediate values (temperature, time, concentration). Thus, the most accurate and efficient synthesis parameters can be achieved. After the experimental studies, using mathematical modeling methods, optimum EMI SE values can be obtained in line with the outputs obtained from the experimental studies, and thus the study can be enriched. Also, with the help of optimization methods, time, raw material, and cost savings can be systematically ensured.

References

1. Song C, Yin X, Han M, Li X, Hou Z, Zhang L, et al. Three-dimensional reduced graphene oxide foam modified with ZnO nanowires for enhanced microwave absorption properties. *Carbon N Y.* 2017;116.
2. Nasouri K, Shoushtari AM. Designing, modeling, and manufacturing of lightweight carbon nanotubes/polymer composite nanofibers for electromagnetic interference shielding application. *Compos Sci Technol.* 2017;145.
3. Geetha S, Kumar KKS, Rao CRK, Vijayan M, Trivedi DC. EMI shielding: Methods and materials - A review. *J Appl Polym Sci.* 2009;112(4).
4. Pang H, Sahu RP, Duan Y, Puri IK. MnFe₂O₄-coated carbon nanotubes with enhanced microwave absorption: Effect of CNT content and hydrothermal reaction time. *Diam Relat Mater.* 2019 Jun 1; 96:31–43.
5. Chen H, Ma W, Huang Z, Zhang Y, Huang Y, Chen Y. Graphene-Based Materials toward Microwave and Terahertz Absorbing Stealth Technologies. *Adv Opt Mater.* 2019;7(8).
6. Pan H, Yin X, Xue J, Cheng L, Zhang L. In-situ synthesis of hierarchically porous and polycrystalline carbon nanowires with excellent microwave absorption performance. *Carbon N Y.* 2016;107.
7. Li H, Lu X, Yuan D, Sun J, Erden F, Wang F, et al. Supporting information Lightweight flexible carbon nanotube/polyaniline films with outstanding EMI shielding property. 2017.
8. Han M, Yin X, Kong L, Li M, Duan W, Zhang L, et al. Graphene-wrapped ZnO hollow spheres with enhanced electromagnetic wave absorption properties. *J Mater Chem A Mater.* 2014 Oct 21;2(39):16403–9.

9. Kokotov M, Hodes G. Reliable chemical bath deposition of ZnO films with controllable morphology from ethanolamine-based solutions using KMnO₄ substrate activation. *J Mater Chem.* 2009;19(23):3847–54.
10. Tunç ID, Erol M, Güneş F, Sütçü M. Growth of ZnO nanowires on carbon fibers for photocatalytic degradation of methylene blue aqueous solutions: An investigation on the optimization of processing parameters through response surface methodology/central composite design. *Ceram Int.* 2020;46(6).
11. Kumar Y, Chopra S, Gupta A, Kumar Y, Uke SJ, Mardikar SP. Low temperature synthesis of MnO₂ nanostructures for supercapacitor application. *Mater Sci Energy Technol.* 2020 Jan 1;3:566–74.
12. Cetinkaya T, Akbulut H, Tokur M, Ozcan S, Uysal M. High capacity Graphene/ α -MnO₂ nanocomposite cathodes for Li–O₂ batteries. *Int J Hydrogen Energy.* 2016 Jun 22;41(23):9746–54.
13. Deng W, Li T, Li H, Dang A, Liu X, Zhai J, et al. Morphology modulated defects engineering from MnO₂ supported on carbon foam toward excellent electromagnetic wave absorption. *Carbon N Y.* 2023 Mar 25;206:192–200.
14. Wang L, Xing H, Gao S, Ji X, Shen Z. Porous flower-like NiO@graphene composites with superior microwave absorption properties. *J Mater Chem C Mater.* 2017;5(8):2005–14.
15. Wang L, Xing H, Gao S, Ji X, Shen Z. Porous flower-like NiO@graphene composites with superior microwave absorption properties. *J Mater Chem C Mater.* 2017;5(8).
16. Song C, Yin X, Han M, Li X, Hou Z, Zhang L, et al. Three-dimensional reduced graphene oxide foam modified with ZnO nanowires for enhanced microwave absorption properties. *Carbon N Y.* 2017 May 1;116:50–8.
17. Chen C, Chen W, Zong B, Ding X, Dong H. Component controllable of graphene/NiO composite with superior shielding of microwave wave ability based on dielectric dissipation. *Journal of Materials Science: Materials in Electronics.* 2020 Nov 1;31(22):20539–48.

18. Pozar_Microwave Engineering(2012) kitap.
19. Chung DDL. Materials for electromagnetic interference shielding. Vol. 255, Materials Chemistry and Physics. Elsevier Ltd; 2020.
20. Aydın KB. Development of Electromagnetic Wave Absorption Properties of Graphene-Based Nanocomposites by Using Stochastic Optimization Methods. 2023.
21. Shahzad F, Alhabeab M, Hatter CB, Anasori B, Hong SM, Koo CM, et al. Electromagnetic interference shielding with 2D transition metal carbides (MXenes) [Internet]. Available from: <http://science.sciencemag.org/>
22. Chen D, Quan H, Huang Z, Luo S, Luo X, Deng F, et al. Electromagnetic and microwave absorbing properties of RGO@hematite core-shell nanostructure/PVDF composites. *Compos Sci Technol.* 2014;102.
23. Wang T, Li Y, Wang L, Liu C, Geng S, Jia X, et al. Synthesis of graphene/ α -Fe₂O₃ composites with excellent electromagnetic wave absorption properties. *RSC Adv.* 2015;5(74):60114–20.
24. Qian J, Du B, He C, Cai M, Zhong X, Ren S, et al. Morphology-controlled preparation and tunable electromagnetic wave absorption performance of manganese dioxide nanostructures. *Journal of the American Ceramic Society.* 2022;105(5).
25. Li JS, Huang H, Zhou YJ, Zhang CY, Li ZT. Research progress of graphene-based microwave absorbing materials in the last decade. Vol. 32, *Journal of Materials Research.* 2017.
26. Aydın KB, Aydın L, Güneş F. Modeling and Optimum Design of Carbon Nanotube/Polyvinyl Alcohol Hybrid Nanofibers as Electromagnetic Interference Shielding Material. *Integr Mater Manuf Innov.* 2022 Sep 1;11(3):391–406.
27. Gong C, Lee G, Shan B, Vogel EM, Wallace RM, Cho K. First-principles study of metal-graphene interfaces. *J Appl Phys.* 2010 Dec 15;108(12).
28. Yang S, Xu D wei, Chen P, Qiu H fang, Guo X. Synthesis of popcorn-like α -Fe₂O₃/3D graphene sponge composites for excellent microwave absorption properties by a facile

- method. *Journal of Materials Science: Materials in Electronics*. 2018 Nov 1;29(22):19443–53.
29. Zhang Z, Xiao F, Qian L, Xiao J, Wang S, Liu Y. Facile synthesis of 3D MnO₂-graphene and carbon nanotube-graphene composite networks for high-performance, flexible, all-solid-state asymmetric supercapacitors. *Adv Energy Mater*. 2014 Jul 15;4(10).
 30. Xu D, Xiong X, Chen P, Yu Q, Chu H, Yang S, et al. Superior corrosion-resistant 3D porous magnetic graphene foam-ferrite nanocomposite with tunable electromagnetic wave absorption properties. *J Magn Magn Mater*. 2019 Jan 1;469:428–36.
 31. Peng T, Si Y, Qian J, Zhang Z, Yan X, Zhu C, et al. Reduced graphene oxide/MnFe₂O₄ nanocomposite papers for fast electrical heating and microwave absorption. *Appl Surf Sci*. 2023;613.
 32. Sankaran S, Deshmukh K, Ahamed MB, Khadheer Pasha SK. Recent advances in electromagnetic interference shielding properties of metal and carbon filler reinforced flexible polymer composites: A review. Vol. 114, *Composites Part A: Applied Science and Manufacturing*. Elsevier Ltd; 2018. p. 49–71.
 33. Liang J, Wang Y, Huang Y, Ma Y, Liu Z, Cai J, et al. Electromagnetic interference shielding of graphene/epoxy composites. Vol. 47, *Carbon*. 2009. p. 922–5.
 34. Pradhan S, Goswami D, Ghorai SK, Ratna D, Chattopadhyay S. Excellent electromagnetic interference shielding and mechanical properties accomplished in a manganese dioxide decorated graphene/polymer composite. *J Appl Polym Sci*. 2021;138(32).
 35. Singh AK, Prasad J, Kumar A, Srivastava A, Tyagi UP, Prajapati B, et al. One-step facile synthesis of MoS₂ - reduced graphene oxide/ZnO nanostructure for high-performance microwave absorption. *Mater Sci Eng B Solid State Mater Adv Technol*. 2023 Jul 1;293.
 36. Li X, Li Z, Que L, Ma Y, Zhu L, Pei C. Electromagnetic wave absorption performance of Graphene/SiC nanowires based on graphene oxide. *J Alloys Compd*. 2020 Sep 15;835.

37. Zhao D, Yuan X, Li B, Jiang F, Liu Y, Zhang J, et al. Silicon carbide nanowire covered by vertically oriented graphene for enhanced electromagnetic wave absorption performance. *Chem Phys*. 2020 Jan 15;529.
38. Quan L, Qin FX, Estevez D, Wang H, Peng HX. Magnetic graphene for microwave absorbing application: Towards the lightest graphene-based absorber. *Carbon N Y*. 2017 Dec 1;125:630–9.
39. Xia Y, Gao W, Gao C. A Review on Graphene-Based Electromagnetic Functional Materials: Electromagnetic Wave Shielding and Absorption. Vol. 32, *Advanced Functional Materials*. John Wiley and Sons Inc; 2022.
40. Zhang X, Zhang X, Yuan H, Li K, Ouyang Q, Zhu C, et al. CoNi nanoparticles encapsulated by nitrogen-doped carbon nanotube arrays on reduced graphene oxide sheets for electromagnetic wave absorption. *Chemical Engineering Journal*. 2020 Mar 1;383.
41. Liu P, Huang Y, Yan J, Yang Y, Zhao Y. Construction of CuS Nanoflakes Vertically Aligned on Magnetically Decorated Graphene and Their Enhanced Microwave Absorption Properties. *ACS Appl Mater Interfaces*. 2016;8(8).
42. Meng F, Wang H, Huang F, Guo Y, Wang Z, Hui D, et al. Graphene-based microwave absorbing composites: A review and prospective. Vol. 137, *Composites Part B: Engineering*. Elsevier Ltd; 2018. p. 260–77.
43. Chen H, Huang Z, Huang Y, Zhang Y, Ge Z, Qin B, et al. Synergistically assembled MWCNT/graphene foam with highly efficient microwave absorption in both C and X bands. *Carbon N Y*. 2017;124.
44. Kong L, Yin X, Yuan X, Zhang Y, Liu X, Cheng L, et al. Electromagnetic wave absorption properties of graphene modified with carbon nanotube/poly(dimethyl siloxane) composites. *Carbon N Y*. 2014;73:185–93.
45. Liu Z, Pan F, Deng B, Xiang Z, Lu W. Self-assembled MoS₂/3D worm-like expanded graphite hybrids for high-efficiency microwave absorption. *Carbon N Y*. 2021 Apr 15;174:59–69.

46. Güneş F, Aykaç A, Erol M, Erdem Ç, Hano H, Uzunbayir B, et al. Synthesis of hierarchical hetero-composite of graphene foam/ α -Fe₂O₃ nanowires and its application on glucose biosensors. *J Alloys Compd.* 2022 Feb 25;895.
47. Geim AK. Graphene: Status and Prospects [Internet]. Available from: <http://science.sciencemag.org/>
48. Geim AK, Novoselov KS. The rise of graphene [Internet]. Available from: www.nature.com/naturematerials
49. Allen MJ, Tung VC, Kaner RB. Honeycomb carbon: A review of graphene. *Chem Rev.* 2010 Jan 13;110(1):132–45.
50. Dong X, Wang X, Wang J, Song H, Li X, Wang L, et al. Synthesis of a MnO₂-graphene foam hybrid with controlled MnO₂ particle shape and its use as a supercapacitor electrode. *Carbon N Y.* 2012 Nov;50(13):4865–70.
51. Dong X, Wang X, Wang J, Song H, Li X, Wang L, et al. Synthesis of a MnO₂-graphene foam hybrid with controlled MnO₂ particle shape and its use as a supercapacitor electrode. *Carbon N Y.* 2012 Nov;50(13):4865–70.
52. Chang J, Jin M, Yao F, Kim TH, Le VT, Yue H, et al. Asymmetric supercapacitors based on graphene/MnO₂ nanospheres and graphene/MoO₃ nanosheets with high energy density. *Adv Funct Mater.* 2013 Oct 1;23(40):5074–83.
53. Chen Y, Li J, Li T, Zhang L, Meng F. Recent advances in graphene-based films for electromagnetic interference shielding: Review and future prospects. *Carbon N Y.* 2021;180.
54. Yue HY, Zhang HJ, Huang S, Lu XX, Gao X, Song SS, et al. Highly sensitive and selective dopamine biosensor using Au nanoparticles-ZnO nanocone arrays/graphene foam electrode. *Materials Science and Engineering C.* 2020 Mar 1;108.
55. Jehad AK, Yurddaskal M, Gunes F, Zafer C, Kocabas K. Investigation of graphene-based Schottky junction solar cell with heavy-doped silicon. *Journal of Materials Science: Materials in Electronics.* 2021 Dec 1;32(24):28856–69.

56. Chen Z, Xu C, Ma C, Ren W, Cheng HM. Lightweight and flexible graphene foam composites for high-performance electromagnetic interference shielding. *Advanced Materials*. 2013 Mar 6;25(9):1296–300.
57. Cao X, Shi Y, Shi W, Lu G, Huang X, Yan Q, et al. Preparation of novel 3D graphene networks for supercapacitor applications. *Small*. 2011 Nov 18;7(22):3163–8.
58. Banciu CA, Nastase F, Istrate AI, Veca LM. 3D Graphene Foam by Chemical Vapor Deposition: Synthesis, Properties, and Energy-Related Applications. Vol. 27, *Molecules*. MDPI; 2022.
59. Hou T, Wang B, Jia Z, Wu H, Lan D, Huang Z, et al. A review of metal oxide-related microwave absorbing materials from the dimension and morphology perspective. Vol. 30, *Journal of Materials Science: Materials in Electronics*. Springer New York LLC; 2019. p. 10961–84.
60. Gao T, Glerup M, Krumeich F, Nesper R, Fjellvåg H, Norby P. Microstructures and spectroscopic properties of cryptomelane-type manganese dioxide nanofibers. *Journal of Physical Chemistry C*. 2008 Aug 28;112(34):13134–40.
61. Song H, Xu L, Chen M, Cui Y, Wu CE, Qiu J, et al. Recent progresses in the synthesis of MnO₂ nanowire and its application in environmental catalysis. Vol. 11, *RSC Advances*. Royal Society of Chemistry; 2021. p. 35494–513.
62. Ding B, Zheng P, Ma P, Lin J. Manganese Oxide Nanomaterials: Synthesis, Properties, and Theranostic Applications. Vol. 32, *Advanced Materials*. Wiley-VCH Verlag; 2020.
63. Wang X, Ni S, Zhou G, Sun X, Yang F, Wang J, et al. Facile synthesis of ultra-long α -MnO₂ nanowires and their microwave absorption properties. *Mater Lett*. 2010;64(13).
64. Song L, Duan Y, Liu J, Pang H. Insight into electromagnetic absorbing performance of MnO₂ from two dimensions: Crystal structure and morphology design. *Mater Charact*. 2020 May 1;163.

65. Wu Y, Liu Y, Wang W, Wang J, Zhang C, Wu Z, et al. Microwave absorption enhancement and loss mechanism of lamellar MnO₂ nanosheets decorated reduced graphene oxide hybrid. *Journal of Materials Science: Materials in Electronics*. 2019 Jan 15;30(1):842–54.
66. Zhang Z, Wang S, Lv Y, Chen X, Wu Z, Zou Y. MnO₂ nanostructures deposited on graphene foams for broadband and lightweight electromagnetic absorption. *J Alloys Compd*. 2019 Nov 25;810.
67. Aydin L, Artem HS, Oterkus S. *Designing Engineering Structures Using Stochastic Optimization Methods*. 1st ed. Vols. 1–9, *Designing Engineering Structures Using Stochastic Optimization Methods*. CRC Press; 2020.
68. Cavazzuti M. *Optimization methods: From theory to design scientific and technological aspects in mechanics*. *Optimization Methods: From Theory to Design Scientific and Technological Aspects in Mechanics*. 2013.
69. Lan B, Sun M, Lin T, Cheng G, Yu L, Peng S, et al. Ultra-long α -MnO₂ nanowires: Control synthesis and its absorption activity. *Mater Lett*. 2014;121.
70. Tran TS, Tripathi KM, Kim BN, You IK, Park BJ, Han YH, et al. Three-dimensionally assembled Graphene/ α -MnO₂ nanowire hybrid hydrogels for high performance supercapacitors. *Mater Res Bull*. 2017;96.
71. Guan H, Chen G, Zhang S, Wang Y. Microwave absorption characteristics of manganese dioxide with different crystalline phase and nanostructures. *Mater Chem Phys*. 2010;124(1).
72. Qian J, Du B, He C, Cai M, Zhong X, Ren S, et al. Morphology-controlled preparation and tunable electromagnetic wave absorption performance of manganese dioxide nanostructures. *Journal of the American Ceramic Society*. 2022 May 1;105(5):3339–52.
73. Dong X, Wang X, Wang J, Song H, Li X, Wang L, et al. Synthesis of a MnO₂-graphene foam hybrid with controlled MnO₂ particle shape and its use as a supercapacitor electrode. *Carbon N Y*. 2012 Nov;50(13):4865–70.

74. Chung DDL. Materials for electromagnetic interference shielding. Vol. 255, Materials Chemistry and Physics. Elsevier Ltd; 2020.
75. Fallah Madvari R, Hosseinabadi S, Bidel H, Pourtaghi G, Laal F. Total Shielding Efficiency, Reflection Loss and Absorption Loss of Nanoparticles/Paraffin Wax Absorber in the Shielding of Electromagnetic Pollution. Transactions on Electrical and Electronic Materials. 2022 Dec 1;23(6):666–73.
76. Li Y, Wang J, Zhang Y, Banis MN, Liu J, Geng D, et al. Facile controlled synthesis and growth mechanisms of flower-like and tubular MnO₂ nanostructures by microwave-assisted hydrothermal method. J Colloid Interface Sci. 2012;369(1).
77. Shah HU, Wang F, Javed MS, Ahmad MA, Saleem M, Zhan J, et al. In-situ growth of MnO₂ nanorods forest on carbon textile as efficient electrode material for supercapacitors. J Energy Storage. 2018;17.
78. Dresselhaus MS, Jorio A, Saito R. Characterizing graphene, graphite, and carbon nanotubes by Raman spectroscopy. Annu Rev Condens Matter Phys. 2010 Jul;1:89–108.
79. Bai XL, Gao YL, Gao ZY, Ma JY, Tong XL, Sun H Bin, et al. Supercapacitor performance of 3D-graphene/MnO₂ foam synthesized via the combination of chemical vapor deposition with hydrothermal method. Appl Phys Lett. 2020 Nov 2;117(18).
80. Wang WX, Liang SH, Yu T, Li DH, Li YB, Han XF. The study of interaction between graphene and metals by Raman spectroscopy. In: Journal of Applied Physics. 2011.
81. Li H, Lu X, Yuan D, Sun J, Erden F, Wang F, et al. Lightweight flexible carbon nanotube/polyaniline films with outstanding EMI shielding properties. J Mater Chem C Mater. 2017;5(34):8694–8.
82. Zhang, L., Liu, M., Bi, S., Yang, L., Roy, S., Tang, X. Z., ... & Hu, X. Polydopamine decoration on 3D graphene foam and its electromagnetic interference shielding properties. Journal of colloid and interface science. 2017;493:327-333.

Appendices

Appendix A

Publications from the Thesis

Conference Papers

1. G. F. Yavuz, K. B. Aydın F. Güneş, Investigation of Seeding Layer Effect on the Growth of MnO₂ Nanowires on Graphene Foam via Simple Hydrothermal Method, 16 th Nanoscience and Nanotechnology Conference (NANOTR 16)16), Ankara, Turkey, September 2022
2. G. F. Yavuz, F. Güneş, The Graphene/TiO₂ Modified PMMA Nanofiber Synthesis with Electrospinning Technique, 5 th International Students Science Congress Proceedings, May 2021
3. G.F. Yavuz, H. Gergerođ lu, F. Güneş, M. Erol, A Simple and Cost Effective Way of Synthesis Hydrophobic Graphene Masks in The Fight Against Covid 19, 3 rd National Carbon Conference, March 2021

Projects

1. General Research Project (National), İzmir Kâtip Çelebi University, Turkey

Project Title: Synthesis and Optimization of Graphene based Nanocomposite as Electromagnetic Wave Absorber

Awards

1. 2210/C National MSc /MA Scholarship Program in the Priority Fields in Science and Technology

Curriculum Vitae

Name Surname: Gülperi Feyza YAVUZ

Education

MSc (2020-2023) - Materials Science and Engineering, İzmir Kâtip Çelebi University

BSc (2014-2020) - Materials Science and Engineering, İzmir Kâtip Çelebi University

Work Experience

08/2019–09/2019 – R&D Engineer (Internship) / Budin Akarca, İzmir, Turkey

08/2018–09/2018 – Production Engineer (Internship) / Şafak Döküm, İzmir, Turkey

Scholarship

(2021 – 2022)- 2210/C National MSc/MA Scholarship Program in the Priority Fields in Science and Technology

Publication

Şen, M., Azizi, E., Avcı, İ., Aykaç, A., Ensarioğlu, K., Ok, İ., Yavuz, G.F., & Güneş, F. (2022), Screen Printed Carbon Electrodes Modified with 3D Nanostructured Materials for Bioanalysis: A Comparison Study, *Electroanalysis*.
<https://doi.org/10.1002/elan.202100624>

Conferences and Proceedings

-L. Çolakoğlu, G. F. Yavuz, M. Savran, H. Parlak and L. Aydın, Modelling and Optimization of Process Parameters During Turning of Aluminum 6061 Using Neuro-Regression Analysis, 1st International Conference on Trends in Advanced Research (ICTAR), Konya, Turkey, March 2023

-G. F. Yavuz, K. B. Aydın, F. Güneş, Investigation of Seeding Layer Effect on the Growth of MnO₂ Nanowires on Graphene Foam via Simple Hydrothermal Method, 16th Nanoscience and Nanotechnology Conference (NANOTR-16), Ankara, Turkey, September 2022

-G. F. Yavuz, F. Güneş, The Graphene/TiO₂ Modified PMMA-Nanofiber Synthesis with Electrospinning Technique, 5th International Students Science Congress Proceedings, May 2021

-G. F. Yavuz, H. Gergeroğlu, F. Güneş, M. Erol, A Simple and Cost-Effective Way of Synthesis Hydrophobic Graphene Masks In The Fight Against Covid-19, 3rd National Carbon Conference, March 2021

-G. F. Yavuz, L. Aydın, M. Savran, H. Sayı, H. S. Artem, Stochastic Optimization of Friction Stir Welded AA7039 Aluminum Alloy Joints Using Neuro-Regression Approach for Maximum Tensile Strength, 4th International Students Science Congress, September 2020

-G. F. Yavuz, M.Ö. Seydibeyoğlu, Surface Modification at Reinforcing Fibers for Elastomer Composites, International Conference on Materials Science, Mechanical and Automotive Engineerings and Technology (IMSMATEC), June 2019